THE ROLE OF REVERSIBLE PROTEIN PHOSPHORYLATION IN THE GLIDING MOTILITY OF *MYCOPLASMA PNEUMONIAE*

by

CLINTON AVERY PAGE

(Under the direction of DUNCAN CHARLES KRAUSE)

ABSTRACT

Mycoplasma pneumoniae exhibits a novel form of gliding motility along solid/liquid interfaces, which may be a virulence factor, necessary for colonization of the respiratory epithelium of human hosts. Given that genes known to be involved in gliding in other organisms are absent in the *M. pneumoniae* genome, random transposon mutagenesis was employed to generate mutants with gliding-deficient phenotypes. Transposon insertions in the only annotated ser/thr kinase (*prkC*; MPN248) and its cognate phosphatase (*prpC*; MPN247) in *M. pneumoniae* resulted in significant and contrasting effects on gliding frequencies. *prkC* mutants glided at approximately half the frequency of wild-type cells, while *prpC* mutants glided more than twice as frequently as wild-type cells. The combined application of Western immunoblotting and Pro Q Diamond phosphoprotein staining identified several proteins as potential targets for PrkC phosphorylation. These included HMW1 and HMW2, which localize to the *M. pneumoniae* terminal organelle, are essential for the assembly of this structure, and have

been previously shown to contain phosphoserine and phosphothreonine, as well as the major adhesin protein P1. In order to confirm the correlation between phosphorylation / dephosphorylation and gliding frequency, the *prkC* and *prpC* mutants were complemented with wild-type copies of their respective disrupted alleles by transposon delivery. Gliding frequencies and phosphorylation levels returned to the wild-type standard in the complemented *prpC* mutant. Surprisingly, the recombinant wild-type *prkC* allele dramatically increased gliding frequency in the *prkC* mutant to a level approximately three-fold greater than that in wild-type. Experiments in which phosphate was removed from the gliding medium showed that gliding frequency was reduced in wild-type cells, but not affected in *prpC* and *prkC* mutants, while the replacement of glucose with glycerol as a carbon source suggested that the regulation of gliding is tied to the phosphotransferase system. Collectively these data suggest that PrkC and PrpC work in opposition in *M. pneumoniae* to influence gliding frequency.

INDEX WORDS: *Mycoplasma pneumoniae*, gliding motility, protein phosphorylation, *prpC*, *prkC*, terminal organelle

THE ROLE OF REVERSIBLE PROTEIN PHOSPHORYLATION IN THE GLIDING MOTILITY OF *MYCOPLASMA PNEUMONIAE*

by

CLINTON AVERY PAGE

B.S., University of South Carolina, 2002

A Dissertation Submitted to the Graduate Faculty of The University of Georgia in Partial Fulfillment of the Requirements for the Degree

DOCTOR OF PHILOSOPHY

ATHENS, GEORGIA

2012

THE ROLE OF REVERSIBLE PROTEIN PHOSPHORYLATION IN THE GLIDING MOTILITY OF *MYCOPLASMA PNEUMONIAE*

by

CLINTON AVERY PAGE

Major Professor:	Duncan C. Krause
Committee:	Mark A. Farmer Timothy R. Hoover Eric V. Stabb

Electronic Version Approved:

Maureen Grasso

Dean of the Graduate School

The University of Georgia

May 2012

TABLE OF CONTENTS

Page

LIST OF TABLES

Page

LIST OF FIGURES

Page

CHAPTER 1

INTRODUCTION

Mycoplasma pneumoniae is a cell wall-less bacterial pathogen of the human respiratory tract that causes primary atypical pneumonia and tracheobronchitis (Waites and Talkington, 2004). *M. pneumoniae* and related organisms lack major biosynthetic pathways, classical transcriptional regulators, chemotactic and other two component systems, and the prototypical prokaryotic cell division apparatus (Himmelreich *et al*., 1996). The limited biosynthetic capabilities of mycoplasmas are generally explained by their evolution as obligate parasites of diverse eukaryotic hosts (Brown, 2002). Colonization of the host by *M. pneumoniae* requires gliding motility (Jordan *et al*., 2007), which may facilitate access to the respiratory epithelium and perhaps lateral spread as infections progress.

The gliding mechanism of *M. pneumoniae* is confined to a polar terminal structure (Hasselbring and Krause, 2007) that also functions in cell division (Hasselbring *et al*., 2006a) and adhesion to host receptors (Hu *et al*., 1982). While the adhesin proteins P1 and P30 localize to the terminal organelle and function in gliding (Hasselbring *et al*., 2005 and Seto *et al*., 2005a), mutant analysis also shows that these proteins are essential for cytadherence and attachment to surfaces. Accordingly, their distinct functions in gliding motility are difficult to define by mutagenesis alone. Given that the genome of *M. pneumoniae* exhibits no homology to defined gliding mechanisms (Himmelreich *et*

al., 1996 and Dandekar *et al*., 2000), including those of other gliding mycoplasmas (Seto *et al*., 2005b, Uenoyama *et al*., 2004 and Uenoyama and Miyata, 2005), it was necessary to perform saturating transposon mutagenesis in order to identify components specific to gliding (Hasselbring *et al*., 2006b). Transposon insertions in the genes encoding the cytoskeletal proteins P41 and P65 (Regula *et al*., 2001), which localize to the terminal structure of *M. pneumoniae* (Hasselbring *et al*., 2006a), produced gliding deficient phenotypes (Hasselbring and Krause, 2007 and manuscript in preparation), but the defect in each is not clearly associated with an actual gliding motor and suggests little about its structure and function. Gliding-deficient phenotypes were also found to result from transposon interruption of genes encoding putative lipoproteins and ABC transporters, as well as genes with metabolic functions and several hypothetical genes (Dandekar *et al*., 2000). One of the most striking gliding mutant phenotypes observed was the "lawn-like" satellite growth of mutants resulting from transposon interruption of the open reading frames (ORF) MPN247 and MPN254 (Hasselbring *et al*., 2006b). These genes encode PrpC, the sole annotated protein phosphatase in the *M. pneumoniae* genome and a component of the phosphotransferase system (PTS) in *M. pneumoniae* (Dandekar *et al*., 2000 and Halbedel *et al*., 2006) and CinA, a protein implicated in competence induction in *Streptococcus pneumoniae* (Lee and Morrison, 1999).

PrpC is a member of a family of serine/threonine phosphatases termed "eukaryotic-like" (eSTPs) despite a growing recognition of their ubiquity in eubacteria. PrpC and its homologs are often partnered with cognate kinases belonging to a family of highly conserved eukaryotic-like serine/threonine kinases (eSTKs). Mutant analysis in *B. subtilis* has shown that homologs to these enzymes regulate sporulation and cell wall

development by reversible phosphorylation (Absalon *et al*., 2009 and Shah *et al*., 2010). Similar reversible phosphorylation may occur in *M. pneumoniae*, in which PrkC and PrpC are reportedly responsible for the phosphorylation and dephosphorylation, respectively, of the terminal organelle proteins HMW1, HMW3 and P1 (Schmidl *et al*., 2009).

Insertion mapping of transformants from a related study (Hasselbring *et al*., 2006a) yielded a serendipitous transposon interruption in MPN248, which encodes PrpC's cognate kinase PrkC (Fig. 1). The catalytic region of PrkC in this mutant, designated 248-377, is intact and should remain functional, but gliding in this mutant occurred at roughly half the frequency of wild-type. Furthermore, phosphorylation of HMW1 and HMW2 as assayed by Pro Q Diamond staining was reduced below wild-type levels in this mutant. Complementation of the *prpC* mutant by transposon delivery of the recombinant wild-type allele restored gliding speed and frequency to the wild-type standard. However, the recombinant copy of *prkC* dramatically increased the frequency of gliding in complemented transformants of the *prkC* mutant approximately three-fold above that of wild-type.

The data presented in this dissertation provide evidence that PrpC and PrkC contribute to the regulation of gliding in *M. pneumoniae* by the reversible phosphorylation of terminal organelle proteins.

CHAPTER 2

REVIEW OF THE LITERATURE

Taxonomy and evolutionary history of the *Mollicutes*

The *Mollicutes* are best known for their small genomes (0.58 to 2.2 megabases), which quite possibly approximate a minimal genetic complement necessary to sustain bacterial life (Glass, 2006), and for their lack of a peptidoglycan cell wall. This latter characteristic is the primary argument for the removal of the mollicutes from a class within the *Firmicutes* to their own phylum ("*Tenericutes*"), though genomic sequencing has found that the *Mollicutes* (both names denote a "soft-skinned" organism) share closer ancestry with the *Clostridia* than either group does with the *Bacilli* or *Streptococci* (Henz *et al*, 2005). The *Taxonomic Outline of Bacteria and Archaea* and *Bergey's Manual of Systematic Biology* continue to differ on this issue, with *Bergey's* recommending the phyletic distinction (Brown, 2007).

Phylogenetic analysis indicates that the ancestors of the *Mollicutes* appeared approximately 600 million years ago (Maniloff, 2002). Given that the first eukaryotic multicellular life appeared approximately concurrently (Shen, 2008), it is tempting to speculate that the availability of multicellular hosts spurred the evolution of early *Mollicutes* as parasitic organisms, though a recent hypothesis actually speculates that the mutation and eventual loss of genes associated with cell shape and division, as the

inaugural evolutionary event in the development of mollicutes (Mitchell Balish, personal communication). Briefly, this process is thought to have begun with the loss of *mreB* as a determinant of cell shape, followed by *spo0J*, *divIVa*, the *min* system and most of the *fts* genes.

The earliest diverging *Mollicutes* species probably resembled members of the modern genus *Acholeplasma* more closely than other extant genera, given some metabolic similarities to *Streptococci*, the lack of a sterol requirement for growth, and the usage of the opal stop codon (UGA) to code for tryptophan rather than stop (Inamine *et al*., 1990) which is a common trait in the "SEM" branch of *Mollicutes* (*Spiroplasmataceae*, *Entoplasmataceae* and *Mycoplasmataceae*), thought to have diverged later. As mentioned earlier, the *Mollicutes* are generally parasitic, though some behave commensally (Taylor-Robinson, 1996) and lack many of the biosynthetic capabilities (along with the associated genes) common to free-living bacteria, such as the synthesis of nucleotides and amino acids, two-component regulatory systems and transcriptional regulators (Fraser *et al*, 1995 and Himmelreich *et al*, 1996). The evolution of the *Mollicutes* is therefore often considered "reductive", though the complex adaptations individual species have made to persist in their hosts regularly belie that assumption.

Initial isolation and classification

The first of the *Mollicutes* to be isolated was the etiologic agent of contagious bovine pleuropneumonia (Nocard and Roux, 1896). The cause of this disease was determined by a clever experiment in which pulmonary fluid from infected animals was used to successfully inoculate semi-permeable pouches of sterile medium incubated in the peritoneal cavity of live rabbits. Serial cultures could be grown from inoculated media and were capable of re-infecting cattle, while heat treatment annulled viability, establishing the described condition as a biological infection. Further study indicated that this organism was a bacterium rather than a virus, as it was capable of growing in cell-free medium (Bordet, 1910), and that it had the unusual property of being able to pass through a 150 nm filter (Elford, 1929). Similar bacteria, identified as the causative agents of respiratory disease in domesticated animals and humans, were discovered afterward and categorized as "pleuropneumonia-like organisms" or PPLOs (Sabin, 1941).

Nocard and Roux's isolate eventually came to be known as *Mycoplasma mycoides* (Edward and Freundt, 1956), due to the fungal appearance of its colonies (from the Greek "mykes" and "plasma"; "fungus-formed"). "Mycoplasma" was initially a catch-all term for PPLOs and other filterable bacterial species, though it currently refers specifically to a single genus within the family *Mycoplasmataceae*, whose members are obligate parasites of vertebrates. *Mycoplasma pneumoniae* is a pathogen of the human respiratory system and the most thoroughly studied of the mycoplasmas, and indeed of the *Mollicutes*.

Early studies of *Mycoplasma pneumoniae*

M. pneumoniae was identified as an etiologic agent of primary atypical pneumonia (PAP), colloquially known as "walking pneumonia", by Eaton and colleagues (1945), but was thought to be a viral pathogen until experiments established that "Eaton's agent" was susceptible to streptomycin and tetracycline (Marmion and Goodburn, 1961). Shortly thereafter, *M. pneumoniae* was cultivated in cell-free culture and described as a PPLO (Chanock *et al*., 1962). Subsequently, the ability of *M. pneumoniae* to attach to the tracheal epithelium of several vertebrate hosts was suggested as a virulence factor in PAP (Sobeslavsky *et al*., 1968).

A survey of gliding motility in PPLOs found that *M. pneumoniae* was one of a subset of PPLOs that displayed gliding on liquid-solid interfaces (Bredt, 1968). Later studies showed that *M. pneumoniae* cells glide in the direction of a polar tip structure leading a thicker "body" segment and ending in a longer "tail" (Bredt, 1973). This polar structure was also shown to be the point of contact between individual *M. pneumoniae* cells and host epithelium (Collier and Clyde, 1974). The discovery of this convergence of adherence and gliding function in the tip structure, later referred to as the "attachment organelle" or "terminal organelle", remains the single most important finding in the study of *M. pneumoniae* cell biology and provided an understanding of how cells infect and persist in the host epithelium.

Pathogenesis

M. pneumoniae is the etiologic agent of 15-20% of community-acquired pneumonia, though infection most commonly manifests as tracheobronchitis (Waites and Talkington, 2004). Colonization of the host begins with inhalation of droplets spread as aerosols (Clyde, 1979) and requires attachment to the respiratory epithelium (Krause *et al*., 1982) implying the necessity of successful transit of the mucociliary layer. While only three percent of infections result in atypical pneumonia (Clyde, 1993), there is a significantly increased incidence in older children and in the elderly (Luby, 1991, Ferwerda *et al*., 2001). In the event that atypical pneumonia develops, symptoms appear within 1-3 weeks of inhalation, most commonly sore throat, fever and a non-productive dry cough, although chills, chest discomfort and headache are not unusual (Ferwerda *et* al., 2001 and Talkington *et al*., 2001). Approximately 20% of infections are asymptomatic (Clyde, 1993).

M. pneumoniae is also implicated as a causative agent in approximately 5% of cases of Guillain-Barré Syndrome (Jacobs, 2002), an autoimmune disorder of the peripheral nervous system. Occurrence of the syndrome can manifest in the wake of a respiratory tract infection by *M. pneumoniae* (Hodges and Perkins, 1969), a common gateway for other rare, but serious extrapulmonary manifestations (Waites and Talkington, 2004). The contribution of *M. pneumoniae* to asthma via induction of inflammatory mediators has been documented as well (Sutherland and Martin, 2007 and Waites and Talkington, *et al.*, 2004).

The hemolytic activity of *M. pneumoniae* colonies when overlaid with blood, attributed to the production of reactive oxygen species (ROS) (Cohen and Somerson, 1967) was long thought to be the primary means by which the symptoms of tracheobronchitis and eventual pneumonia were generated during colonization of host epithelia. This hypothesis is supported by the reduced cytotoxicity of mutants lacking the glycerophosphodiesterase GlpQ, which is implicated in the production of ROS as a byproduct of phosphatidylcholine metabolism (Schmidl *et al.*, 2011).

Following annotation of the *M. pneumoniae* genome, the ORF MPN372 was identified as having homology to the S1 subunit of the exotoxin produced by *Bordetella pertussis* (Dandekar *et al*., 2000) and investigated for potential cytotoxicity. The recombinant, synthesized protein product of MPN372 functions in ADP-ribosylation (Kannan and Baseman, 2006), as does its homologous subunit in the pertussis toxin, and has been shown to generate an inflammatory response in baboons and mice (Hardy, *et al*., 2009). CARDS (Community Acquired Respiratory Disease Syndrome) toxin, as it came to be known, has also been detected in the damaged airways of *M. pneumoniae*-infected mice (Kannan *et al*., 2011).

M. pneumoniae **genetics**

The genome of *M. pneumoniae* is a single chromosome of 816,394 base pairs, representing approximately 700 protein coding genes (Himmelreich *et al*., 1996 and Dandekar *et al*., 2000). In addition to the aforementioned absence of genes involved in cell division, biosynthetic and regulatory pathways, *M. pneumoniae* also lacks several

genes required for DNA repair in other organisms, among them the *mut* genes involved in response to oxidative stress and some SOS genes; this may contribute to the elevated rate of mutation in *M. pneumoniae* and its reductive evolution. The lack of a complete copy of *recA* in the *M. pneumoniae* was long considered to be a barrier to site-directed mutagenesis of specific genes, though recent experiments by Krishakumar and colleagues (2010) suggest that specific gene knockouts are possible. Random transposon mutagenesis by the modified *Staphylococcus aureus* transposon TN4001.2065 and its derivatives (Knudtsen and Minion, 1993, Hahn *et al*., 1999 and Zimmerman and Herrmann, 2005) is the best means for generating mutants and delivering recombinant DNA constructs to the genome.

An unexpected finding in the genomic analysis of *M. pneumoniae* does not concern specific genes but intergenic sequences. While the Pribnow box (the short sequence approximately 10 bases upstream of transcriptional start sites in *Eubacteria*) is present in mycoplasmas, the partner sequence approximately 35 bases upstream of the transcription site, as well as Shine-Dalgarno ribosome binding sites cannot be identified.

M. pneumoniae biochemistry

A defined medium has recently been established as a minimal medium for cell-free growth of *M. pneumoniae* (Yus *et al*., 2009); this medium includes glucose and glycerol as carbon sources (glycerol appears to be essential for growth), all nucleobases, cholesterol, several fatty acids with Bovine Serum Albumin as a carrier molecule, nine vitamins and co-factors, and all but two amino acids (aspartate and glutamate are synthesized from asparagine and glutamine), again highlighting the limited biosynthetic

capabilities of the organism. *M. pneumoniae* ferments glucose (and is capable of fermenting other monosaccharides) by the Embden-Meyerhoff pathway, producing lactate as an end product. It has been suggested that in the limited nutritional environment of the host respiratory epithelium, *M. pneumoniae* cells may derive at least some of their carbon and energy requirements from the catabolism of glycerophospholipids sloughed off the host cell membrane. The glycolytic intermediate glycerol-3-phosphate can be derived from enzymatic degradation of these molecules and could hypothetically enter directly into glycolysis (Schimdl *et al*., 2011).

The *M. pneumoniae* terminal organelle and its components

The initial studies of *M. pneumoniae* gliding referenced earlier (Bredt, 1973) described the cell body of *M. pneumoniae* as having a leading tip followed by a wider cell body and a long tail-like segment. Transmission electron microscopy of this terminal organelle revealed an internal framework with a longitudinally oriented structure at its center, commonly referred to as the "electron-dense core". A terminal "button" at the distal end of the electron-dense core (relative to the cell body) was also observed (Biberfeld and Biberfeld, 1970 and Wilson and Collier, 1976). Subsequent experiments identified rods of corresponding length to the electron-dense core in Triton X-100 fractions, suggesting that the core and its accessory components constituted a cytoskeleton (Gobel *et al*., 1981). A series of thin filaments extending from the proximal (to the cell body) end of the electron-dense core through the cell body was also observed (Meng and Pfister, 1981).

In recent years, electron cryotomography has presented a much clearer picture of the terminal structure. The core of the *M. pneumoniae* terminal organelle was shown to consist of a pair of angled rods, one longer and thicker than the other, bordered at the proximal end by a bowl-shaped structure separating the terminal structure from the cell body (Henderson and Jensen, 2006 and Seybert *et al*., 2006) (Fig. 14A). At the date of this writing, the individual components of the *M. pneumoniae* cytoskeleton are not identified with specific proteins, though a number of cytoskeletal proteins associated with the core have been identified, along with their orientation relative to the core (Regula *et al*., 2001, Balish *et al*., 2003, Bose *et al*., 2009).

P1, B and C: Following the determination that the terminal organelle was involved in the adhesion of *M. pneumoniae* cells to the respiratory epithelium of the host, trypsinization of live mycoplasma cells revealed that an extracellular protein with a molecular mass of 170 kilodalton (kDa) was responsible for attachment to host receptors, specifically to sialoglycoconjugates (Powell *et al*., 1976 and Hu *et al*., 1977). Immunoferritin electron microscopy employing antibody to this protein, designated P1, showed clustering of immunoferritin/antibody/P1 complexes at the terminal organelles of wild-type cells, but not at the terminal organelles of non-adherent mutants (Baseman, *et al*., 1982, Feldner *et al*., 1982 and Hu *et al*., 1982), while antibody inhibition of adherence to hamster tracheal ring cells, controlling for cytotoxicity effects on *M. pneumoniae* cells, demonstrated that P1 was indeed the primary adhesin (Krause and Baseman, 1983).

P1 is encoded by the ORF MPN141, and is co-transcribed with the downstream ORF MPN142, which encodes two separate proteins of 90 kDa and 40 kDa, respectively (Inamine *et al*., 188 and Layh-Schmitt and Herrmann, 1992). These proteins, commonly referred to as B and C, were shown to localize to the interior of the cell membrane, in the terminal organelle, and in close proximity to P1 (Layh-Schmitt and Herrmann, 1994), suggesting a supporting role for P1 function.

In addition to its role in cytadherence, P1 also functions in the gliding motility of *M. pneumoniae*. Cells gliding in borosilicate growth chambers ceased gliding and actually detached from the gliding substrate following the addition of P1 antibody to the gliding medium, while non-motile cells remained attached, indicating that specific surface moieties of P1 may be exposed during gliding but not while resting (Seto *et al*., 2005a). It has been suggested that P1 works (along with protein B) as a "leg protein" in gliding motility, functioning comparably to the Gli proteins of *Mycoplasma mobile* (Nakane *et al*., 2011), though currently available data only establishes a linkage between P1 and B when they are co-isolated from whole cells via gel filtration and native PAGE.

P30 and P65: Protein P30 is also a surface-exposed *M. pneumoniae* adhesin that localizes to the terminal organelle but does not appear to attach to surfaces in a sialic acid- dependent manner (Krause *et al*., 1982, Baseman *et al*, 1987 and Chang *et al*., 2011). Like P1, P30 has a secondary role in gliding (Hasselbring *et al*., 2005) and is associated with an intracellular accessory protein, P65 (Proft *et al*., 1995 and Jordan *et al*., 2001). P30 and P65 are among the last of the terminal organelle proteins to assemble in a newly formed terminal organelle (Hasselbring *et al*., 2006a).

P41 and P24: P41 is a cytoskeletal protein localizing to the proximal end of the terminal organelle (Hasselbring *et al*, 2006a). Transposon disruption of the ORF encoding P41 (MPN311) resulted in mutant strain that attached to erythrocytes and glass at wild-type levels, but exhibited an aberrant, filamentous satellite growth phenotype, suggesting that P41 had a function in gliding motility but not attachment. While mutants were altered in the gliding phenotype (Hasselbring *et al*., 2006b), these mutants were distinguished by a striking feature; the terminal organelles of mutant cells were observed to detach from the cell body and glide independently, establishing that the gliding motor of *M. pneumoniae* is located within the terminal organelle (Hasselbring and Krause, 2007). P24 is encoded by the ORF downstream of MPN311 and partners with P41 in the development of new terminal organelles (Hasselbring *et al*., 2007).

HMW1, HMW2 and HMW3: The three "High Molecular Weight" (HMW) proteins of *M. pneumoniae* are essential for cytadherence (Baseman *et al*., 1982, Krause *et al*., 1982, Hahn *et al*., 1998 and Willby and Krause, 2002) but do not function as adhesins. Rather, each of these proteins is required for the assembly of the terminal organelle and the proper localization of adhesins and their accessory proteins (Krause and Balish, 2004). HMW1 and HMW2 are reciprocally dependent and are thought to be required very early in the assembly of new terminal organelles; in the absence of either, the core of the terminal organelle cannot form. While HMW3 is not required for the formation of the core or the stability of HMW1 and HMW2, mutant analysis indicates that the HMW3 is essential for proper orientation of the core and for the localization of P30 and P65 (Willby and Krause, 2002). The P1/B/C complex can only properly localize in the terminal organelle following the precise assembly of the preceding components.

HMW1 and HMW2 are both phosphorylated in an ATP-dependent manner at serine and threonine residues (Dirksen *et al*., 1994 and Krebes *et al*., 1995). While the specific effect of phosphorylation of these proteins is not known, it seems feasible that in the absence of traditional transcriptional regulators, post-translational modification may have an important role in the assembly sequence of new terminal organelles.

Gliding motility in *M. pneumoniae*

The original studies of *M. pneumoniae* gliding referenced earlier (Bredt, 1973) described *M. pneumoniae* cells gliding at approximately 0.3 μm / second during observation periods and occasionally reaching speeds of 2.0 μm / second for limited times. Gliding was also noted to cease irregularly for resting periods representing between 0 and 80% of the observation period (Radestock and Bredt, 1977). Modern studies of wild-type cells largely concur with these findings and also include the percentage of cells gliding during observation, or gliding frequency, as approximately 28% (Hasselbring *et al*., 2006b).

Studies of gliding in a normal human bronchial epithelium (NHBE) model indicate that gliding may be a virulence factor for *M. pneumoniae*. Gliding mutants lacking protein P200 (MPN567) were clearly deficient in colonization of respiratory epithelium relative to wild-type, while complementation with P200 returned colonization to wild-type levels. Significantly, the P200 mutant attached at wild-type levels to A549 cells and erythrocytes but exhibited significantly reduced gliding velocity, suggesting that failure to colonize NHBE cells was a function of the gliding defect (Jordan *et al*., 2007).

NHBE modeling of *M. pneumoniae* colonization is a robust system and should contribute significant clarification to this issue in the coming years.

Gliding motility is more definitively associated with cell division in *M. pneumoniae.* Shortly after the first experiments quantifying gliding motility in *M. pneumoniae*, Bredt (1968) documented the classic pattern of terminal organelle-assisted cytokinesis, in which a cell ceased gliding and developed a second tip structure adjacent to the original. One of the tip structures would slowly migrate to the other cell pole before the daughter cells separated. This phenomenon was investigated in further detail by experiments in which newly formed terminal organelles appeared to migrate, presumably under the power of the gliding motor, to an opposite cell pole along with replicated chromosomes. However, as these experiments required fixation for DAPI staining and immunofluorescence assays, a continuous sequence of events was not available for consideration (Seto *et al.*, 2005b). A study of division employing live cells, in which the location of new terminal organelles was detected by fluorescent protein fusions to terminal organelle proteins, confirmed the earlier hypothesis and established that gliding deficient mutants were also impaired in cell division (Hasselbring *et al.*, 2006a). Additionally, this study showed that, at least during *in vitro* culture, cell division regularly involves the formation of several new terminal organelles before cytokinesis is observed.

While P1 and P30 certainly function in *M. pneumoniae* gliding, no mechanism internal to the terminal organelle presents itself as a likely motor for gliding. The components of better understood gliding mechanisms such as those of *Myxococcus xanthus* (Goldman *et al*., 2006) and *Flavobacterium johnsoniae* (McBride *et al*., 2009)

share no homology with *M. pneumoniae*. The proposed mechanism of P1-driven phase-dependent motility (Nakane *et al.,* 2011) cannot be evaluated for the same reason. Studies of the terminal organelle and its components by cryotomography are continuing, and may represent the best means to identify the gliding motor.

Reversible Protein Phosphorylation in *M. pneumoniae*

In the decade following the sequencing of the *M. pneumoniae* genome, the study of signal transduction in relation to the regulation of cellular processes in other organisms expanded rapidly. The Min system of *Escherichia coli* (Shapiro and Losick, 2000) as well as quorum sensing, biofilm formation and chemotaxis in multiple bacterial species (Miller and Bassler, 2001, Karatan and Watnick, 2009 and Cluzel *et al*., 2000) were not new subjects, but they experienced tremendous growth in a few years, due largely to the increase in computational power that made genomic sequencing possible. Annotation of the *M. pneumoniae* genome (Dandekar *et al*., 2000) dissuaded researchers from investigating similar pathways in mycoplasmas, however, as histidine kinases and other regulatory enzymes and receptor molecules simply had no homology to established signaling cascades.

The first indication that a functioning intracellular signaling system might have an important effect in the development of *M. pneumoniae* was the identification of altered satellite growth patterns and deficient gliding motility in association with transposon interruption of the predicted serine / threonine phosphatase *prpC* (Hasselbring *et al.,* 2006b). Shortly thereafter, PrpC was found to exhibit phosphatase activity and to be a component of the PTS in *M. pneumoniae* (Halbedel *et al.,* 2006). Mutation of the

neighboring kinase gene *prkC* produced an unusual mutant in which HMW2, along with other terminal organelle proteins, were absent or reduced in steady state levels, producing a non-adhering phenotype. The authors took this to indicate that the stability of terminal organelle proteins was dependent on serine / threonine phosphorylation (Schmidl *et al*., 2009), though they did not complement the mutant and assure that the phenotype was not the result of a secondary mutation. The phosphoprotein profile of a *prpC* mutant isolated in the earlier PTS study showed that HMW2 and the other terminal organelle proteins present at reduced levels in the *prkC* mutant were hyperphosphorylated, suggesting that reversible phosphorylation by these enzymes was an important regulatory factor in *M. pneumoniae*.

A subsequent study identified more phosphoproteins subject to reversible phosphorylation by *prpC* and *prkC* by a combined application of 2-D gel electrophoresis, fluorescent phosphoprotein staining and mass spectrometry. Profiles indicative of reversible phosphorylation were detected for the terminal organelle proteins HMW3, P65 and P41, along with the cell surface protein encoded by MPN474 and a handful of smaller proteins of unknown function (Table 1), including a fragment of Sigma factor 24 (RpoE) not previously known to be functional (Schmidl *et al*., 2010). An earlier mass spectrometry study investigating phosphorylation in *M. pneumoniae* and the closely related species *Mycoplasma genitalium* identified a similar set of phosphoproteins along with the specific serine and threonine residues at which some proteins are phosphorylated (Su *et al*., 2007).

A recent study has shown that post-translational modification of proteins in *M. pneumoniae* is not limited to serine / threonine phosphorylation. In combination with a

third survey of phosphoproteins by mass spectrometry, van Voort and colleagues (2012) also described the acetylation of lysine residues in the proteome of wild-type *M. pneumoniae* and in two strains in which acetyltransferases were disrupted by transposon insertion. Most strikingly, this study found that the serine / threonine phosphorylation state of a number of *M. pneumoniae* proteins had a clear, but complex effect on the total number of neighboring acetylated lysine residues within those proteins, and vice-versa. For example, thirteen lysine residues were less heavily acetylated in the terminal organelle protein HMW2 of a *prkC* mutant, while similar effects were noted in acetyltransferases mutants with regard to phosphoserine and phosphothreonine sites. The authors correctly assert that cross-talk between the two post-translational modification systems constitutes a much more complex regulatory system than had been previously thought to function in *M. pneumoniae*.

Regulatory functions of eSTP / eSTK pairs

Phosphorylation of serine, threonine and tyrosine residues was first encountered in studies of eukaryotic biochemistry (De Verdier, 1952 and Sutherland *et al*., 1955) and was considered to be a function exclusive to eukaryotic metabolic regulation until the description of an enzyme in *E. coli* capable of phosphorylating and dephosphorylating serines and threonines relatively late in the 20th century (Garnak and Reeves, 1979 and Bakal *et al*., 2000). The highly conserved enzyme classes described here collectively, for the purpose of brevity, as eSTKs and eSTPs, were not detected in prokaryotic species for several more years, (Munoz-Dorado *et al*., 1991 and Kenelly, 2002). With the advent of genome sequencing, hundreds of these enzymes have been identified in bacterial and

archaeal genomes (Galperin *et al*. 2010), establishing that these enzymes should probably not be described as "eukaryotic-like", given their ubiquity and conservation throughout all domains of life (Fig. 13).

The majority of eSTKs in bacteria are cell membrane and cell envelope-associated enzymes (Yeats *et al*., 2002), featuring a cytosolic catalytic domain connected to one or more extracellular PASTA (**p**enicillin-binding **a**nd **s**erine / **t**hreonine kinase-**a**ssociated) domains by a transmembrane segment. These PASTA domains function in a manner not unlike the extracellular sensor domains of histidine kinases in traditional two-component systems, in some cases functioning in a two-step ligand binding / homodimerization process with a role in catalytic domain activation (Barth *et al*., 2010). In *B. subtilis*, the binding of peptidoglycan fragments by the PASTA domain of the eSTK PrkC activates a signaling cascade in which phosphorylation of Elongation Factor G (EF-G) results in the germination of spores (Shah *et al*., 2008).

Many eSTKs are partnered with, and in close genomic proximity to, a cognate phosphatase from one of the recognized eSTP families (Iwanicki *et al*, 2005). The function of individual eSTPs is often more difficult to elucidate than those of their cognate kinases, though in many cases, they are modulators of the autophosphorylation of these kinases (Obuchowski *et al*., 2000 and Osaki *et al*., 2009). In some cases, eSTPs directly dephosphorylate the phosphoprotein substrates of their cognate eSTKs, completing a regulatory circuit. The eSTK / eSTP –based regulation of a proteins that regulate cell shape and cell wall development in *B. subtilis* is a model system, useful for identifying comparable regulatory circuits in other organisms (Absalon *et al*.,2009).

Table 1. *M. pneumoniae* phosphoproteins detected by mass spectrometry. These proteins have been shown to be phosphorylated and/or dephosphorylated by PrkC/PrpC in *M. pneumoniae* or *B. subtilis* (Su *et al*, 2007 and Schmidl *et al*, 2010).

Locus name	**Protein name**	**Protein function**
MPN024	RpoE	Sigma factor 24 fragment
MPN142	P1	Adhesin protein
MPN256	MPN256	Uncharacterized protein
MPN309	P65	Cytoskeletal protein
MPN310	HMW2	Cytoskeletal protein
MPN311	P41	Cytoskeletal protein
MPN447	HMW1	Cytoskeletal protein
MPN453	HMW3	Cytoskeletal protein
MPN474	MPN474	Cell surface protein
MPN665	Tuf	Elongation factor Tu

CHAPTER 3

MATERIALS AND METHODS

Mycoplasma strains and culture conditions

Wild-type *M. pneumoniae* strain M129 (Lipman and Clyde, 1969), cytadherence mutants M6 (Hahn *et al*, 1998), H9 (Hedryda and Krause, 1995), HMW3- (Willby and Krause, 2002), IV-22 (Krause *et al*, 1982), II-3 (Romero-Arroyo, 1999) and the gliding mutant strains 247-100 and 254-70 (Hasselbring *et al*, 2006b) were described previously.

The gliding deficient *prkC* mutant 248-377 was generated serendipitously by transformation of wild-type M129 with a derivative of the transposon vector pMT85 (Hasselbring *et al*, 2006a). Following identification of the transposon insertion site in this strain, the initial transformant stock was filtered, serially diluted and plated on PPLO agar plates to generate progeny colonies for isolation.

Cultures were grown to mid-log phase in SP-4 medium (Tully *et al*, 1977) with the addition of 18 μg/ml gentamicin and 24 μg/ml chloramphenicol where appropriate for antibiotic selection. Qualitative and quantitative hemadsorption assays followed standard procedures (Fisseha *et al*, 1999 and Krause and Baseman, 1982), as did time-lapse analysis of satellite growth (Hasselbring *et al*, 2006b). All reagents used in these studies were purchased from Sigma Chemical Co., (St. Louis, MO) unless otherwise stated.

Identification of transposon-disrupted genes

Transposon insertion sites in 247-100, 248-377 and 254-70 were mapped by sequencing from a site internal to an inverted repeat sequence common to TN4001.2065 and pMT85, employing the primer 3'LacZ2 (Table 2). Briefly, genomic DNA from each strain was digested with HindIII, ligated, and used to transform *Escherichia coli* strain DH5α. Kanamycin resistant transformants (carrying the transposon's copy of *aacA-aphD*, along with the junction of transposon and *M. pneumoniae* DNA) were expanded in liquid culture. Plasmid DNA was collected by Miniprep (Qiagen, Venlo, Netherlands) and sequenced at the Georgia Genomics Facility (Athens, GA.).

Time-lapse analysis of satellite growth and microcolony development

Satellite growth of *M. pneumoniae* mutants was evaluated as previously described (Hasselbring *et al*, 2005) except that magnification was increased to 100X. We quantified microcolony areas microscopically, collecting 100 measurements of microcolony diameter per strain in order to quantify the differences in colony area between wild-type, mutant and complemented strains.

Western immunoblotting

Samples were analyzed by sodium dodecylsulfate-polyacrylamide gel electrophoresis (SDS-PAGE) and Western immunoblotting as described previously

(Laemmli, 1970 and Towbin *et al*, 1979) using a monoclonal P30-specific antibody (1:1000) (Romero-Arroyo *et al*, 1999) and rabbit antisera to HMW1 (1:10,000) (Stevens and Krause *et al*, 1991), HMW2 / P28 (1:2,000) (Krause *et al*, 1997), HMW3 (1:10,000) (Stevens and Krause, 1992), P1 (1:2,000) (Baseman *et al*, 1982), P200 (1:2,000) (Proft *et al*, 1996), TopJ (1:2,000) (Cloward and Krause, 2009), P65 (1:3,000) (Proft and Herrmann, 1994), B (1:5,000) and C (1:1,000) (Sperker *et al*, 1991), P41 (1:1,000) and P24 (1:250) (Krause *et al*, 1997).

Quantitation of cell gliding

Previous studies described a procedure to measure *M. pneumoniae* gliding frequency and velocity (Hasselbring *et al*, 2005), but a modification to this protocol improved the precision of these measurements, especially in the more fragile mutant strains. Cultures were inoculated approximately 24 h prior to the capture of images for analysis and grown to a cell density of 75-150 cells per field. This technique removed the need for the destructive thawing and needle passage steps used in the previous protocol. In addition, 10 min prior to the capture of images, we replaced the spent medium in which the cultures were inoculated with a defined gliding medium (20 mM HEPES, 150 mM NaCl, 1.0 mM sodium phosphate monobasic, 0.8 mM glucose and gelatin [3% w/v], pH 7.2). This was necessary because gliding measurements in SP-4 with 3% gelatin (Hasselbring *et al*, 2005 and Hasselbring *et al*, 2006b) appeared to vary with the batch of some media components. Wild-type gliding speed and frequency as measured in the defined gliding medium were comparable to previously published values (Hasselbring *et al*, 2005).

In other gliding experiments a phosphate-free gliding medium (recipe as above, omitting sodium phosphate monobasic) was used, as well as a gliding medium in which glucose was replaced with glycerol at a concentration of 0.8 mM. Image capture for measurement of gliding frequency was made 10 min after replacement of growth medium, as above, and once more, 2 h after the initial measurement.

Intrinsic ^{32}P incorporation and autoradiography

Wild-type and mutant *M. pneumoniae* cells were grown in 40 mL of SP-4 in 162 cm^2 tissue culture flasks and harvested during exponential growth. Strains that adhere well to plastic were scraped from the flask surface prior to centrifugation, and all strains were harvested by centrifugation at 20,000 RPM. Cell pellets were washed three times with Tris-buffered saline (TBS) and suspended by needle passage in 250 μL of TBS. Protein concentration of each sample was measured in triplicate by BCA protein assay and adjusted to a final concentration of 1 μg/μl in phosphate-free, pyruvate-free Dulbecco's Modified Eagle's Medium, 20 mM HEPES containing 10% fetal bovine serum dialyzed against TBS. Radiolabeled phosphoric acid ($H_3{}^{32}PO_4$ at 8,500-9120 Ci/mmol; Perkin Elmer, Waltham, MA) was added to 1 ml of *M. pneumoniae* suspension in a 1.5 mL microcentrifuge tube to a final concentration of 90 μCi/mL. Cultures were incubated at 37° C with agitation for 12 h, after which cells were harvested and washed with TBS by centrifugation. Pellets were suspended in 1 mL TBS to maintain the concentration of 1 μg/μl. 30 μg of treated sample was analyzed on 5% polyacrylamide gels, blotted to nitrocellulose and exposed to Kodak Biomax XAR film (Rochester, NY) at -80° C in the presence of an intensifier screen for 120 h.

Phosphoprotein staining

Pro Q Diamond stain (Life Technologies, Carlsbad, CA) was used to identify phosphoproteins in wild-type, mutant and complemented samples and to compare the degree of phosphorylation between strains. 7.5% polyacrylamide SDS-PAGE gels (fortified with Invitrogen Rhinohide Polyacrylamide Gel Strengthener) were stained with Pro Q Diamond following the manufacturer's protocol and imaged on a Typhoon Trio laser scanner (GE Healthcare, Little Chalfont, UK) at 532 nm emission/ 580 nm excitation wavelengths. To confirm equal protein levels per sample, gels were also stained with the fluorescent protein stain Sypro Ruby and imaged at 488 nm emission/ 610 nm excitation wavelengths. ImageJ (Rasband, W.S., ImageJ, U. S. National Institutes of Health, Bethesda, MD, http://rsb.info.nih.gov/ij/, 1997-2009) was used to perform background fluorescence subtraction and densitometric analysis of fluorescence-imaged bands corresponding to HMW1, HMW2 and P1. Final intensity measurements, averaged from three experiments, were normalized to those of wild-type.

Reverse transcriptase PCR

Nucleic acids for RT-PCR were extracted from *M. pneumoniae* cultures at mid-log phase by a chloroform/ethanol extraction (Invitrogen Easy-DNA kit, Carlsbad, CA) and treated with the Ambion DNA-free kit (Naugatuck, CT) to remove contaminating DNA. Primer pairs (Table 2, Fig. 5) were designed to generate multiple PCR products spanning intra- and intergenic regions within the *prpC/prkC* gene cluster (Integrated

DNA Technologies, Coralville, IA). Mycoplasma RNA was reverse transcribed with the Ambion Retroscript kit to produce cDNA for PCR, which was carried out in Easystart 50 reaction tubes (Molecular Bio-Products, San Diego, CA). RT-PCR products, along with positive and negative controls, were visualized by ethidium bromide staining following agarose electrophoresis.

Complementation of 247-100 and 248-377 mutants

MPN247 was amplified from wild-type M129 genomic DNA along with the upstream ORF MPN246 and its promoter to construct a recombinant allele of *prpC* for complementation of 247-100. Forward and reverse primers (246F EcoRV and 247R EcoRV, Table 2) were designed with EcoRV sites providing blunt ends for ligation into the SmaI site of the chloramphenicol-resistance vector pKV104 (Hahn *et al*, 1998). A comparable strategy was used to complement the *prkC* mutant 248-377 with forward and reverse primers flanking MPN248 (248F EcoRV and 249R EcoRV). All PCR products intended for inclusion in complementation vectors were generated with Expand High Fidelity Taq Polymerase (Roche, Penzburg, Upper Bavaria, Germany). Transformation of competent cells by electroporation was described previously (Hedryda *et al*, 1993). Transformants were plated on PPLO agar (Lipman *et al*, 1969) with gentamicin and chloramphenicol. Colonies were carefully picked and expanded in 1 ml SP-4 medium. Individual transformants were screened for a restored wild-type satellite growth phenotype by time-lapse analysis.

Table 2. Description of primers used for RT-PCR, complementation and insertion mapping of transformant strains.

Primer Name	Sequence (engineered restriction sites are underlined)
RT-PCR primers	
246F RT	5'-CCTTAACATCGTCCAGCACTAGTCATGCTT-3'
247F RT	5'-TGTGATGGTTTAGGCGGTTATAAGGGCGGT-3'
247R RT	5'-GAAACGGTAGCAGTGAGGGCTAACAGCTTG-3'
248F RT	5'-CGGTTGGTGTTAAAGGTAGTACAACGCA-3'
248F M01	5'-ATGGCACTAAATTTAAAGATTGGT -3'
248F M26	5'-ATGAACTCTTACCTGTTTTTAGCG -3'
248R RT	5'-AGCGTTACGAATAACAGCGGAAGCAATGCC -3'
Primers for complementation (engineered restriction sites are underlined)	
246F EcoRV	5'-CGTGGCGATATCCATAACCCTGGTGC-3'
247R EcoRV	5'-CAGGTAAGAGGATATCCCGCCTGA-3'
248F EcoRV	5'-CGTGGCGATATCCTGTACAACTTCTTGG-3'
249R EcoRV	5'-GCGACAATGACAGATATCTCAAGGG-3'
Insertion mapping primer	
3'LacZ2	5'-CACTCCAGCCGCTTTCCGGCACCGCTTCT-3'

P1 Immunoprecipitation

Prior to immunoprecipitation of protein P1 from *M. pneumoniae* cell lysates, 500 µl of P1 antibody (Baseman *et al*, 1982) at production bleed strength was mixed with 25 µl of a Protein G Dynabead (Invitrogen) suspension and incubated with shaking at 4° C for 1 h. P1 antibody was then recovered from the Dynabeads by magnetic separation (the beads were discarded). This was necessary to reduce non-specific binding between Protein G Dynabeads and components of P1 antibody solution. *M. pneumoniae* cell suspensions (determined by bicinchoninic acid assay to contain 300 µg of protein) were collected by centrifugation (X g for 20 minutes) and resuspended in the detergent buffer TDSET [10 mM Tris-hydrochloride (pH 7.8), 0.2% (wt/vol) sodium deoxycholate, 0.1% (wt/vol) sodium dodecylsulfate, 10mM tetrasodium EDTA, 1% (vol/vol) Triton X-100] for 30 min at 37°C to solubilize protein P1 (Leith *et al*, 1983). Lysates were then incubated with recovered P1 antibody for 1h at 4° C. Finally, 25 µl of fresh Dynabeads were added to the lysate/antibody mixture and shaken at 4° C for 1h. Dynabeads were recovered from the lysate/antibody mixture by magnetic separation and washed twice with TDSET. Following a 10 min incubation at 68°C in 3X SDS-PAGE sample buffer and a final magnetic separation, precipitate was loaded on SDS-PAGE gels for further analysis.

Antisera to PrkC and PrpC

Peptides reflecting the amino acid sequences of PrpC (MASALVSEVFTKSFTVFDF) and PrkC (LRSDVPVSLENIVFKCTA) were synthesized by Sigma-Genosys (St. Louis, MO), conjugated to Keyhole Limpet Hemocyanin and used to generate polyclonal antibodies from rabbits (Antibodies Incorporated, Davis, CA).

CHAPTER 4

RESULTS

Identification of transposon insertion sites in gliding mutants

A collection of 3,500 transformants was screened for aberrant satellite growth phenotypes in order to identify possible motility mutants. Several distinct phenotypes were observed, characterized and separated into four general categories, one of which featured "lawn-like" growth. In the three transformants that displayed this phenotype, the microcolonies characteristic of wild-type *M. pneumoniae* satellite growth did not develop. Sequencing revealed that two of these transformants were "siblings", in which TN4001.2065 had inserted into an identical site in MPN254, while the other transformant featured an insertion in MPN247 (Hasselbring, 2006b). A separate study of *M. pneumoniae* cell division serendipitously identified another transformant in which a lawn-like growth phenotype was observed (Hasselbring, 2006a); sequencing of this strain identified an insertion in MPN248 (Fig. 1).

Genome annotation of *M. pneumoniae* had previously described MPN247 and MPN248 as homologs of the phosphatase/kinase pair *prpC* and *prkC* from *B. subtilis* (Obuchowski *et al.*, 2000 and Dandekar *et al.*, 2000). A nucleotide BLAST search suggested that MPN254 was homologous to the gene *cinA* in *S. pneumoniae*, which has a proposed function in the induction of genetic competence (Altschul *et al.*, 1997 and

Fig. 1. Schematic of *prpC* / *prkC* / *cinA* gene cluster including ORFs MPN246-MPN254.

Predicted functions are based on the most current *M. pneumoniae* genome annotation (Dandekar *et al*, 2000). Black arrowheads indicate transposon insertion sites.

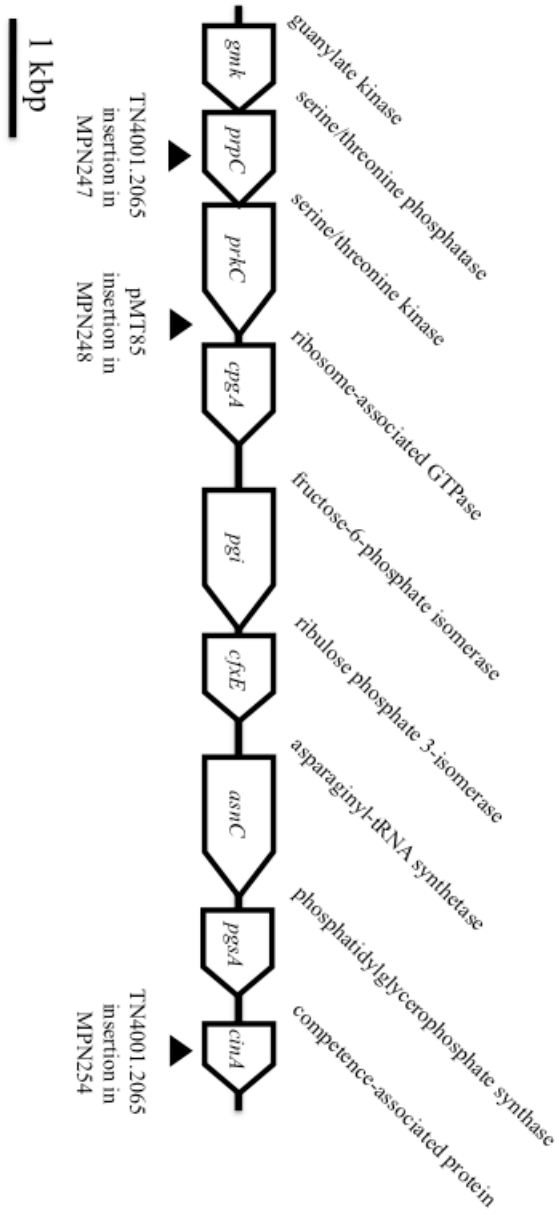
gmk
guanylate kinase
prpC
serine/threonine phosphatase
prkC
serine/threonine kinase
rpgA
ribosome-associated GTPase
pgi
fructose-6-phosphate isomerase
cfxE
ribulose phosphate 3-isomerase
asnC
asparaginyl-tRNA synthetase
pgsA
phosphatidylglycerophosphate synthase
cinA
competence-associated protein
TN4001.2065 insertion in MPN247
pMT85 insertion in MPN248
TN4001.2065 insertion in MPN254
1 kbp

Lee and Morrison, 1999). These mutants were coded 247-100 (*prpC*), 248-377 (*prkC*) and 254-70 (*cinA*); the first number represents the number of the transposon-interrupted ORF, followed by the final canonical amino acid in the truncated protein sequence of each mutant.

General characterization of *prpC*, *cinA and prkC* mutants

The *prpC* and *cinA* mutants 247-100 and 254-70 were previously described (Hasselbring *et al.*, 2006b) as having a lawn-like satellite growth pattern, where the large microcolonies and confluent growth characteristic of wild-type cultures do not form over time (Fig. 2). The pattern observed visually was confirmed here by comparative analysis of average microcolony area, where mutant microcolonies were approximately half the size of wild-type microcolonies at 72 and 96 hours post-inoculation (Table 3). A similar growth pattern was noted for the *prkC* mutant 248-377, both visually (Fig. 2) and in average microcolony area (Table 3), although this mutant achieved confluence more slowly. The observed differences in growth pattern could not be accounted for strictly on the basis of growth rate, although all mutants grew slightly slower than wild-type.

Spontaneous mutations affecting terminal organelle function can arise at a high frequency (Krause and Balish, 2004). Therefore, to explore whether the mutant gliding phenotypes here described were potentially accompanied by secondary mutations, we employed Western immunoblotting to assess steady state levels of proteins known to contribute to cytadherence and/or motility (HMW1, HMW2, HMW3, P1, B, C, P200, TopJ, P65, P41, P24 and P30) revealing that all were present at wild type levels in both the *prpC* mutant 247-100 and the *prkC* mutant 248-377 (Fig. 3).

Fig. 2. Microcolony satellite growth for *prpC* (247-100), *prkC* (248-377) and *cinA* mutants.

Cultures were incubated in chamber slides for 144 h with images captured at 24-h intervals. Scale bars, 15 μm.

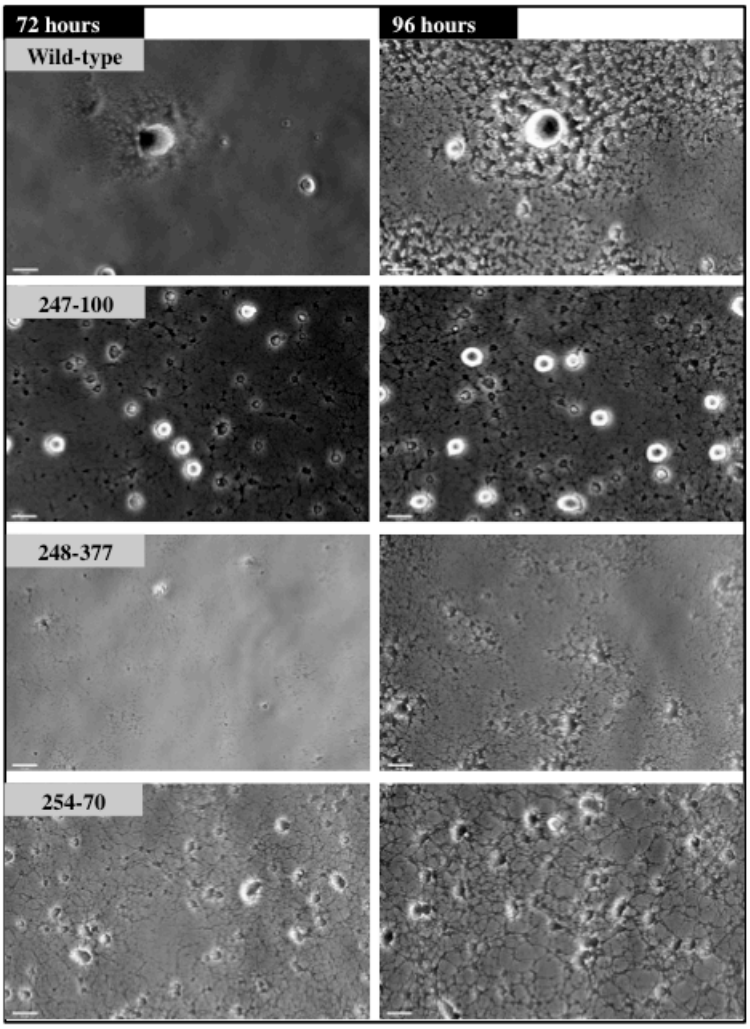
72 hours
96 hours
Wild-type
247-100
248-377
254-70

Table 3. Analysis of satellite growth for wild-type *M. pneumoniae*, *prpC* (247-100), *prkC* (248-377) and *cinA* mutants (254-70) and a complemented *prpC* mutant (247-100 CT1).

Strain	Mean microcolony area[a] at 72 hours	Mean microcolony area[a] at 96 hours
Wild-type	80.65 ± 11.1	116.1 ± 15.6
prpC-	42.56 ± 7.48	49.34 ± 6.54
prpC- C1	82.78 ± 22.3	134.2 ± 41.8
prkC-	32.26 ± 6.54	38.69 ± 7.21
cinA-	41.89 ± 3.56	60.25 ± 4.98

[a] μm^2 ± 95% confidence interval

Fig. 3. Western immunoblot analysis of *prpC* and *prkC* mutants.

20 μg of protein was loaded per lane on a 3-10% polyacrylamide gradient gel. Antisera are indicated to the left.

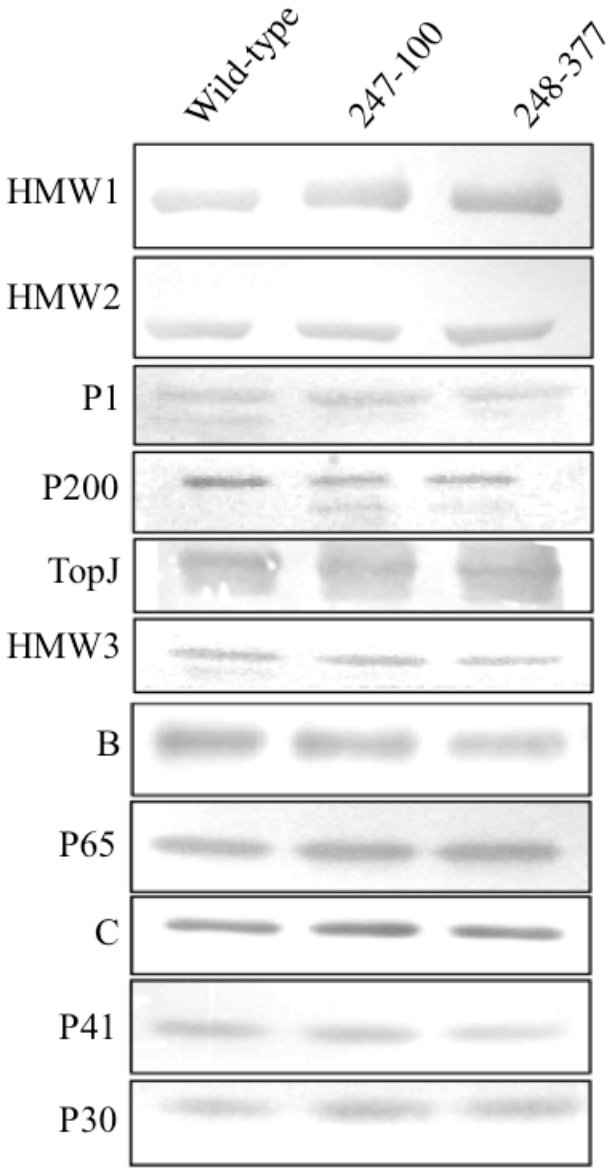
Wild-type
247-100
248-377
HMW1
HMW2
P1
P200
TopJ
HMW3
B
P65
C
P41
P30

Fig. 4. Hemadsorption assays.

A. Qualitative hemadsorption analysis of *prpC* (247-100) and *prkC* (248-377) mutants, with wild-type *M. pneumoniae* and IV-22 (Krause *et* al, 1982) as positive and negative controls, respectively. Scale bars, 65 μm. Insets reflect an approximate threefold magnification.

B. Quantitative hemadsorption analysis, with percent of cells retained normalized to wild-type. Mutant II-3 (Romero-Arroyo, 1999) was used as a negative control. Error bars reflect a 95% confidence interval.

A

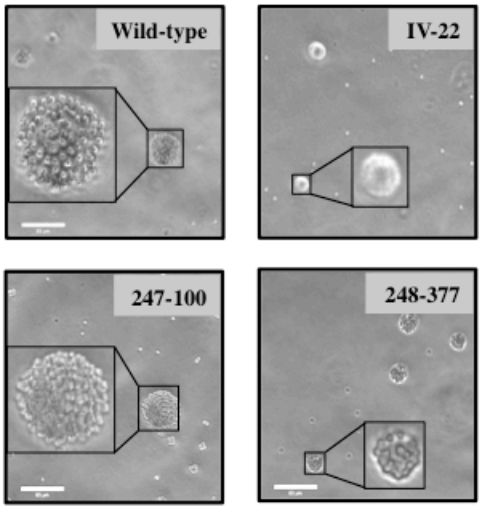
Wild-type
IV-22
247-100
248-377

B

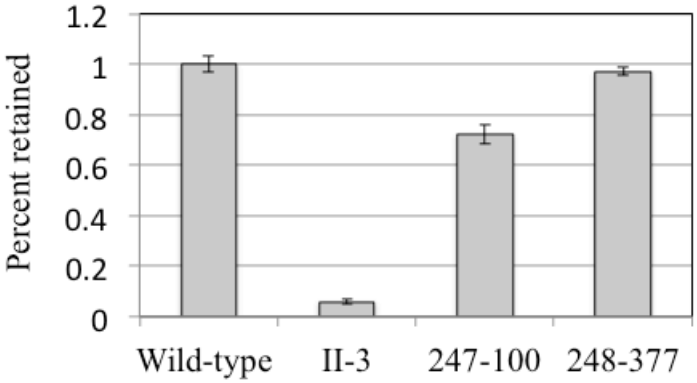
Percent retained
1.2
1
0.8
0.6
0.4
0.2
0
Wild-type
II-3
247-100
248-377

Moreover, qualitative hemadsorption assays confirmed that the transposon disruption of MPN247 or MPN248 did not severely impact cytadherence (Fig. 4A), although the *prpC* mutant attached to erythrocytes at a level approximately 70% of wild-type (Fig. 4B). The protein profile and hemadsorption phenotype of the *cinA* mutant 254-70 were also comparable to wild-type *M. pneumoniae* (data not shown).

Transcription of the *prpC* / *prkC* gene cluster

Reverse transcriptase PCR was employed to identify the most likely locations of promoters in the gene cluster and thereby instruct the strategy for the complementation of mutants 247-100 and 248-377. Two pairs of primers (247F RT / 247R RT and 248F RT / 248R RT, Fig. 5B) were used to amplify intragenic targets of 400 base pairs within MPN247 and MPN248, confirming the presence of transcript from both genes in wild-type *M. pneumoniae* RNA (Fig. 5A, lanes i and ii). A second set of primer pairs (246F RT / 247R RT and 247F RT / 248R RT, Fig. 5B) was used to amplify intergenic targets of 1100 base pairs, the first spanning MPN246 and MPN247, the second spanning MPN247 and MPN248; the transcript spanning MPN246 and MPN247 was amplified following reverse transcription from RNA, but not a transcript spanning MPN247 and MPN248 (Fig 5A, lanes iii and iv). This suggested that a predicted promoter upstream of MPN246 was responsible for transcription of MPN246 and MPN247, while MPN248 was transcribed from a separate sequence within the upstream gene MPN247 (Fig. 5B). However, a possible promoter sequence upstream of a methionine codon 78 nucleotides downstream from the currently annotated start site of MPN248 (Himmelreich *et al.*,

1996) raised the possibility that MPN247 and MPN248 do not overlap but are separated by an intergenic space of approximately 70 nucleotides.

Analysis of transcription within this region employed three forward primers (248F M01, 248F M26 and 248F RT) and one reverse primer (248R RT), producing amplicons of three sizes (Fig. 5D), one identical to the internal *prkC* transcript referenced above (Fig. 5C, lane vii), one corresponding to the currently annotated transcription start site (Fig. 5C, lane ix), and one to the possible upstream start site (Fig. 5C, lane xi). While RT-PCR products were detected for both the currently annotated and hypothetical start sites, the latter produced a much brighter band, which may indicate that the hypothetical start site is the more common site of initiation of transcription for *prkC* (Fig. 5D).

Analysis of gliding motility

Microcinematographic analysis initially determined the gliding frequencies and velocities of mutants 247-100 and 254-70 to be significantly reduced relative to wild-type (Fig. 6). The subsequently isolated strain 248-377 was found to have an even lower gliding frequency (less than 1% of cells gliding per field) than 247-100 and 245-70, precluding analysis of gliding velocity due to a lack of individual gliding cells for measurement. These measurements were based on assays of gliding motility designed for high throughput analysis, utilizing a pre-frozen motility stock and a rapid thaw and syringe passage, which was useful for the purpose of assaying the gliding phenotypes of several dozen mutants given the limits of time and availabilty of personnel. During studies of mutants lacking the cytoskeleton protein P65, a modified protocol for gliding

Fig. 5. RT-PCR analysis of the *prpC/prkC* gene cluster.

A. RT-PCR products of reactions using primers 247F RT and 247R RT (i), 248F RT and 248R RT (ii), 246F RT and 247R RT (iii), and 247F RT and 248R RT (iv). An RT-PCR positive control was loaded in the final lane (v).

B. Schematic detailing the predicted locations of promoters in the *prpC/prkC* gene cluster along with the annealing sites of relevant primers.

C. Products of reactions using primers 248F RT and 248R RT (vi and vii), 248F M01 and 248R RT (viii and ix) and 248F M26 and 248R RT (x and xi). Even-numbered lanes represent positive DNA controls, while odd-numbered lanes are the products of RT-PCR.

D. Schematic detailing MPN248 and its two possible transcription start sites, based on Fig. 5B, along with the annealing sites of relevant primers.

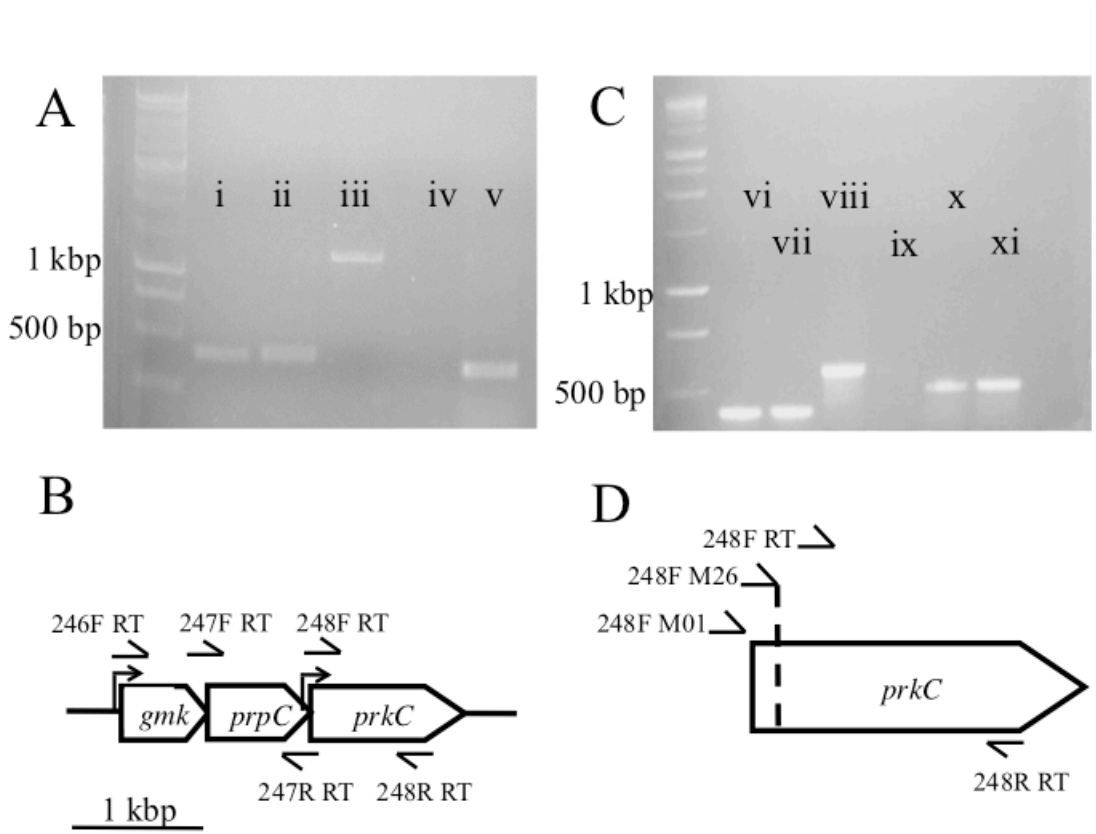
A
i
ii
iii
iv
v
1 kbp
500 bp
C
vi
vii
viii
ix
x
xi
1 kbp
500 bp
B
246F RT
247F RT
248F RT
gmk
prpC
prkC
247R RT
248R RT
1 kbp
D
248F RT
248F M26
248F M01
prkC
248R RT

Fig. 6. Cell gliding frequency and velocity for wild-type *M. pneumoniae*, *prpC*, *prkC* and *cinA* mutants and complemented transformants

A. Mean gliding frequency is a measurement of the number of cells gliding in one observational field divided by the total number of cells in that field. An earlier method of gliding motility analysis (Hasselbring *et al*, 2006b) yielded a mean cell gliding frequency of 2.9% for the *prpC* mutant, less than 1% for the *prkC* mutant and 11% for the *cinA* mutant. One way ANOVA indicated that the differences observed in gliding frequency for the *prpC* and *prkC* mutants, as well as the complimented transformants of the *prkC* mutant, were statistically significant at an α of 0.01. Error bars represent 95% confidence intervals.

B. Mean gliding velocity is measured in μm/s. An earlier method of gliding motility analysis (Hasselbring *et al*, 2006b) yielded a mean gliding velocities of 0.134 μm/s and 0.144 μm/s for the *prpC* and *cinA* mutants respectively. One way ANOVA indicated that the gliding velocity of the *prpC* mutant was significantly greater than that of wild-type.

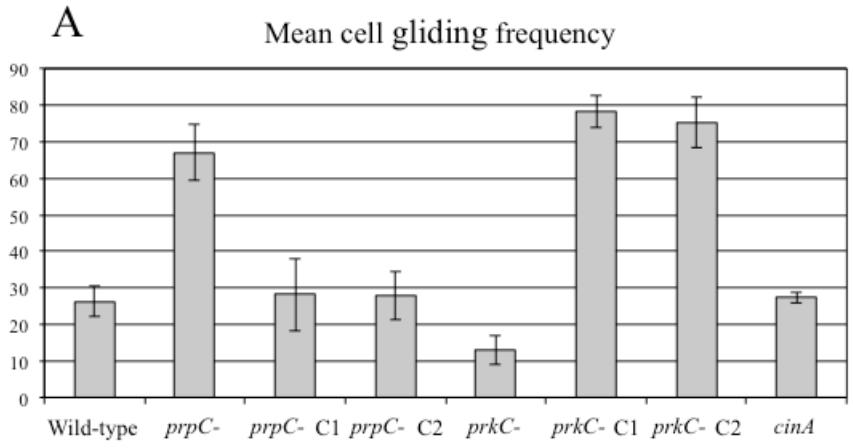
A
Mean cell gliding frequency
90
80
70
60
50
40
30
20
10
0
Wild-type
prpC-
prpC- C1
prpC- C2
prkC-
prkC- C1
prkC- C2
cinA

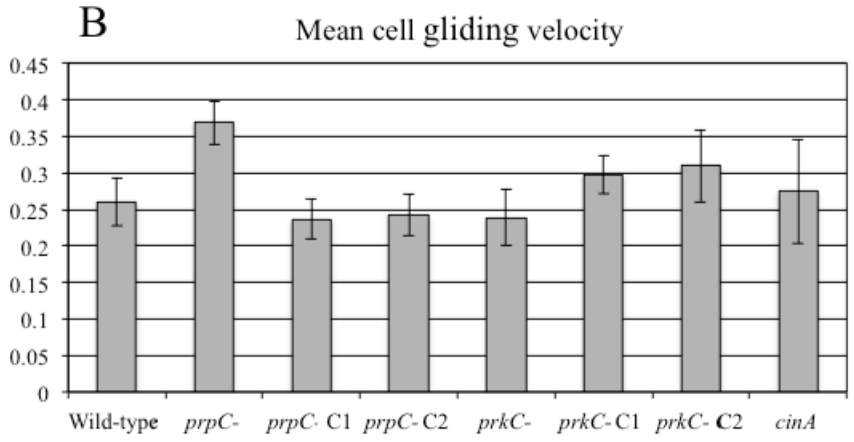
B
Mean cell gliding velocity
0.45
0.4
0.35
0.3
0.25
0.2
0.15
0.1
0.05
0
Wild-type
prpC-
prpC- C1
prpC- C2
prkC-
prkC- C1
prkC- C2
cinA

analysis (discussed in Chapter 3) revealed that while the gliding frequencies and velocities of wild-type cells were essentially equivalent for both rapid and longer-term culture methods, both gliding frequency and velocity in the mutant strains were significantly elevated with the latter method, perhaps due to the destructive effects of thawing and multiple syringe passages.

When gliding was re-evaluated in the *prpC* mutant 247-100 by the longer-term culture method, cells were found to be faster and to glide more than twice as frequently as wild-type cells. In contrast, quantitative motility studies with the *prkC* mutant 248-377 established a gliding frequency approximately half that of wild-type cells, but with comparable gliding speeds, while *cinA* mutant cells were found to glide roughly as frequently and at speeds comparable to wild-type (Fig. 6). The increases in gliding frequency and velocity detected in the *prpC* mutant and the decrease in gliding frequency in the *prkC* mutant were determined to be statistically significant by one-way ANOVA.

Protein phosphorylation in *prkC* and *prpC* mutants

The contrasting gliding phenotypes of mutants 247-100 and 248-377 suggested a role for reversible phosphorylation in *M. pneumoniae* gliding. To study the protein phosphorylation profiles of these mutants we employed $H_3{}^{32}PO_4$ incorporation and autoradiography, as well as Pro Q Diamond phosphoprotein staining.

Radiolabeling of phosphoproteins produced somewhat confounding results. The wild-type phosphorylation profile was comparable to profiles observed in earlier experiments (Dirksen *et al.*, 1994 and Krebes *et al.* 1995), and the profile of the *prkC*

mutant 248-377 reflected apparently lower phosphorylation levels relative to wild-type. However, the profile of the *prpC* mutant 247-100 did not feature the hyperphosphorylation characteristic of other phosphatase mutants (Absalon, 2009), though a band migrating at the size of protein P1 (Fig. 7, box) was more intense in mutant 247-100. Furthermore, in mutant M6, which lacks HMW1 and produces a truncated P30 (Hahn *et al.*, 1998), this putative P1 band likewise appeared to be dramatically hyperphosphorylated relative to wild-type (Fig. 7).

In contrast to the results from ^{32}P incorporation, Pro Q Diamond staining detected hyperphosphorylated bands corresponding to HMW1 and P1 in the *prpC* mutant 247-100, in addition to a modest increase in the intensity of HMW2 relative to wild-type. By comparison, HMW1 and HMW2 bands in the *prkC* mutant 248-377 were consistently less intense than in wild-type, whereas P1 appeared to be phosphorylated at wild-type levels (Fig. 8B). Band intensities were analyzed in triplicate for Pro Q Diamond fluorescence intensity (Fig. 8A), confirming the results noted visually. Sypro Ruby imaging of Pro Q Diamond-stained gels (Fig. 8A) revealed that total protein profiles of the *prpC* (247-100) and *prkC* (248-377) mutants were indistinguishable from wild-type, consistent with Western immunoblotting data (Fig. 3).

We also examined phosphoprotein profiles of the terminal organelle mutant strains M6, H9, HMW3- and IV-22 by Pro Q Diamond staining. The absence of phosphorylated HMW1 or HMW2 in mutants M6 and H9, respectively (Fig. 8B, ovals), was consistent with our previous findings (Dirksen *et al.*, 1994). Interestingly, a band corresponding to truncated HMW2 in mutant H9 (Bose *et al.*, 2009) was also apparent by Pro Q Diamond staining (Fig. 8B, arrowhead). The absence of a phosphorylated band

Fig. 7. Phosphorylation profiles in *prpC, prkC*, HMW1 and HMW2 mutants, assayed by autoradiography. 30 μg of protein, labeled with $H_3{}^{32}PO_4$, was loaded per lane on a 5% polyacrylamide gel and western blotted. Protein P1 in the 247-100 band is indicated by an inset box.

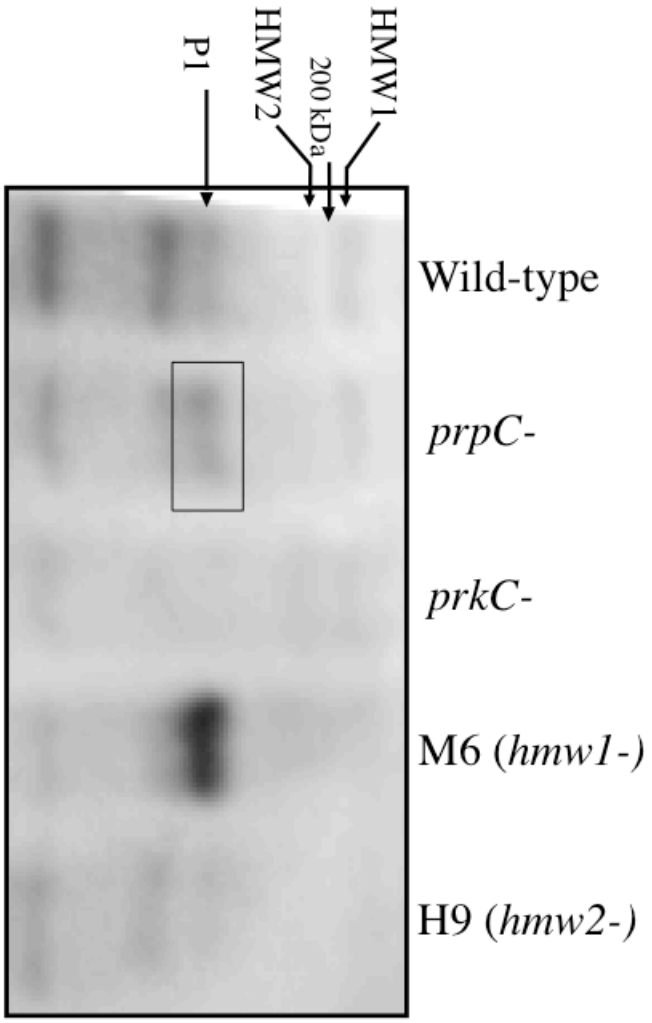
P1
HMW2
200 kDa
HMW1
Wild-type
prpC-
prkC-
M6 (hmw1-)
H9 (hmw2-)

Fig. 8. Phosphorylation profiles in *prpC, prkC*, terminal organelle protein mutants, and complemented transformants assayed by fluorescent phosphoprotein staining.

A. 30 μg of protein was loaded per lane on a 7.5% polyacrylamide gel and stained with Sypro Ruby following electrophoresis to provide total protein profiles.

B. A Pro Q Diamond stain of the same gel.

The 200 kDa protein standard is indicated by arrows, while proteins of interest are indicated by arrowheads. Circles, absence of HMW1 and HMW2 in mutants M6 and H9, respectively; dashed circle, absence of P1 in mutant IV-22; solid arrowhead, likely truncated HMW2 protein in mutant H9.

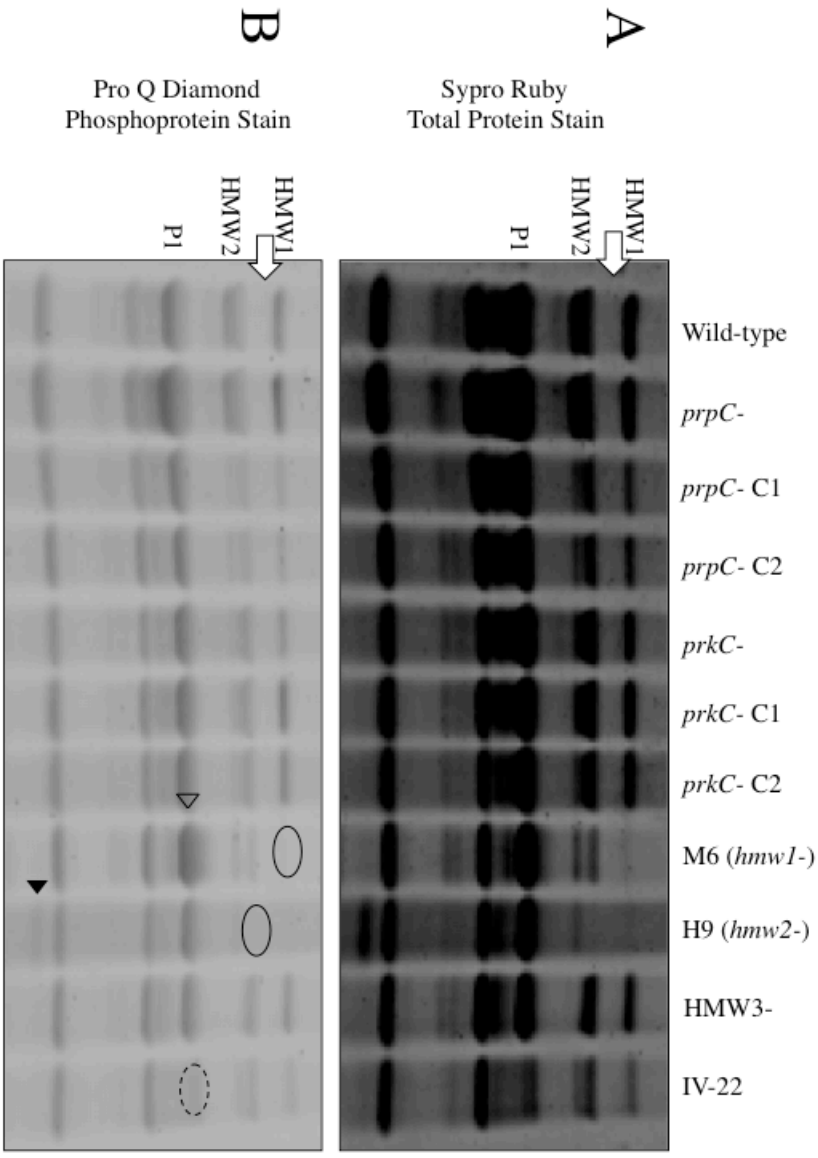
B
Pro Q Diamond
Phosphoprotein Stain
P1
HMW2
HMW1
A
Sypro Ruby
Total Protein Stain
P1
HMW2
HMW1
Wild-type
prpC-
prpC- C1
prpC- C2
prkC-
prkC- C1
prkC- C2
M6 (hmw1-)
H9 (hmw2-)
HMW3-
IV-22

Fig. 9. Relative fluorescence intensity of Pro Q Diamond phosphoprotein staining of bands representing HMW2, HMW1, and P1.

A. Band intensity was determined by densitometric analysis in ImageJ and normalized to wild-type.

B. Bands represent P1 from wild-type and the HMW1 mutant M6, calculated similarly.

All error bars reflect the standard error of the mean, based on three independent experiments.

A

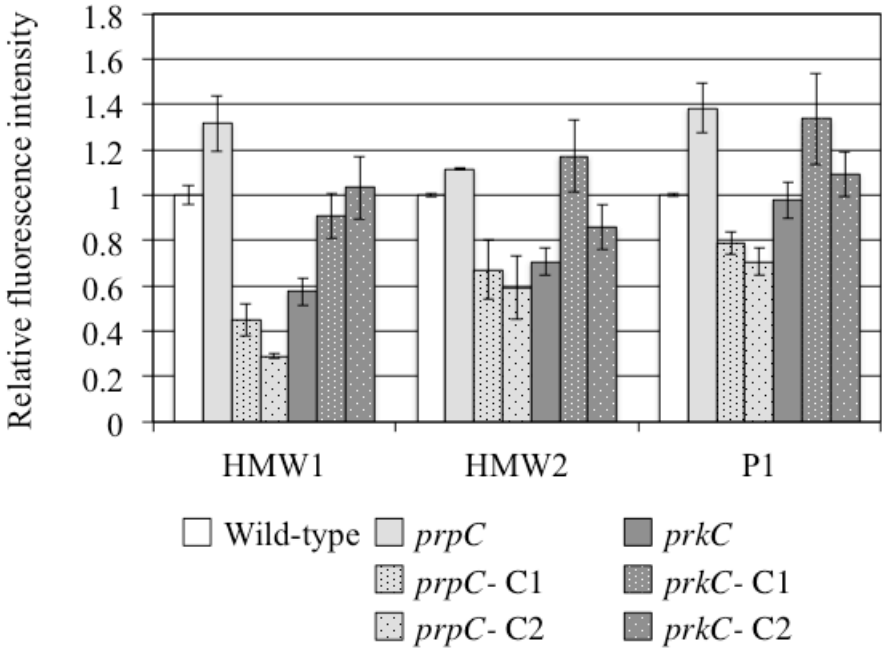
Relative fluorescence intensity
1.8
1.6
1.4
1.2
1
0.8
0.6
0.4
0.2
0
HMW1
HMW2
P1
Wild-type
prpC
prpC- C1
prpC- C2
prkC
prkC- C1
prkC- C2

B

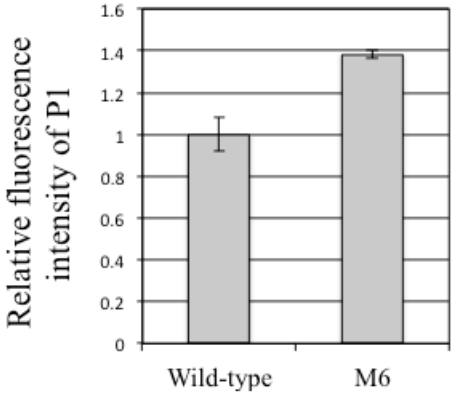
Relative fluorescence intensity of P1
1.6
1.4
1.2
1
0.8
0.6
0.4
0.2
0
Wild-type
M6

corresponding to P1 in mutant IV-22 (Fig. 8B, dashed oval) was likewise consistent with its identification as a phosphoprotein. Hyperphosphorylation of P1 in mutant M6 detected by radiolabeling was also observed by Pro Q Diamond staining (Fig. 8B, open arrowhead and Fig. 9B). We did not detect a difference in band intensity between wild-type and phosphorylation mutants in protein bands resolving at the size of the cytoskeletal protein HMW3, which is described as a phosphoprotein in numerous studies (Su *et al.*, 2007, Schmidl *et al.*, 2009, and Schmidl *et al.*, 2010).

Detection of phosphorylated P1 by immunoprecipitation

To confirm that the hyperphosphorylated band observed in mutant M6 in analysis of protein phosphorylation (Fig. 7 and Fig. 8B) represented the adhesin P1 and not the co-migrating surface protein MPN474, immunoprecipitated P1 from wild-type *M. pneumoniae* and mutant M6 was also stained with Pro Q Diamond (Fig. 10). The immunoprecipitated P1 recovered from M6 also appeared to be hyperphosphorylated relative to wild-type.

Detection of MPN247 and MPN248 gene products

We prepared antisera to peptides corresponding to predicted immunogenic regions of PrpC and PrkC. Antisera to each reacted with the corresponding peptides in dot blots but failed to identify a protein band of the expected size in wild-type profiles but absent in corresponding mutant profiles by Western immunoblotting (data not shown). Attempts at detection following subcellular enrichment were likewise unsuccessful.

Fig. 10. Phosphoprotein staining of immunoprecipitated P1 from wild-type *M. pneumoniae* and HMW1 mutant M6.

Concentrated immunoprecipitate of P1 was loaded on a 7.5% polyacrylamide gel and stained with Pro Q Diamond. Lane #1 is a broad range molecular weight standard.

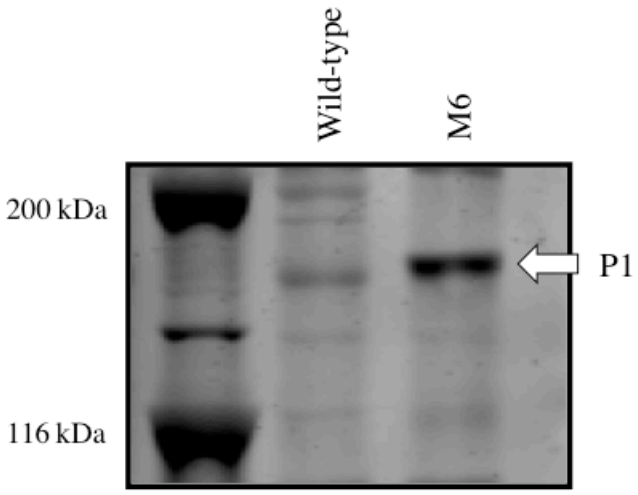
Wild-type
M6
200 kDa
116 kDa
P1

Complementation of *prpC* and *prkC* mutants

Complemented transformants of *prpC* and *prkC* mutants (247-100 CT1/2 and 248-100 CT1/2) were evaluated for restored gliding and phosphorylation phenotypes by microcinematographic analysis and by phosphoprotein staining. The gliding speeds and frequencies of complemented transformants of the *prpC* mutant 247-100 returned to the wild-type standard (Fig. 6). Additionally, the increased phosphorylation of HMW2 and P1 observed in mutant 247-100 was ameliorated by complementation with the wild-type MPN247 allele, (Fig. 8B and Fig. 9A) though phosphorylation of these bands was reduced relative to wild-type (Fig. 9A). Finally, complementation of mutant 247-100 resulted in wild-type satellite growth and an increase in average microcolony area (Table 3). In contrast, complementation data for the *prkC* mutant 248-377 were somewhat confounding, where the delivery of the recombinant wild-type allele resulted in hyperphosphorylation of P1 (Fig. 8B and 9A) and in an increase in gliding frequency to a level even greater than that observed in wild-type and the *prpC* mutant 247-100.

Additional gliding motility experiments

The *prpC* and *prkC* mutants presented an opportunity to explore some aspects of the nutrient requirements and energetics of *M. pneumoniae* gliding. The important role of protein phosphorylation by PrkC in gliding suggested that a gliding medium lacking phosphate might result in a gliding phenotype similar to that of 248-377 in wild-type cells. This was indeed the case, as wild-type cells in phosphate-free media glided at a reduced frequency relative to cells in standard media, while 247-100 and 248-377 glided at comparable rates in both medias (Fig. 11).

Fig. 11. Analysis of wild-type, *prpC* and *prkC* mutant gliding frequencies in phosphate-free gliding media.

Error bars represent a 95% confidence interval.

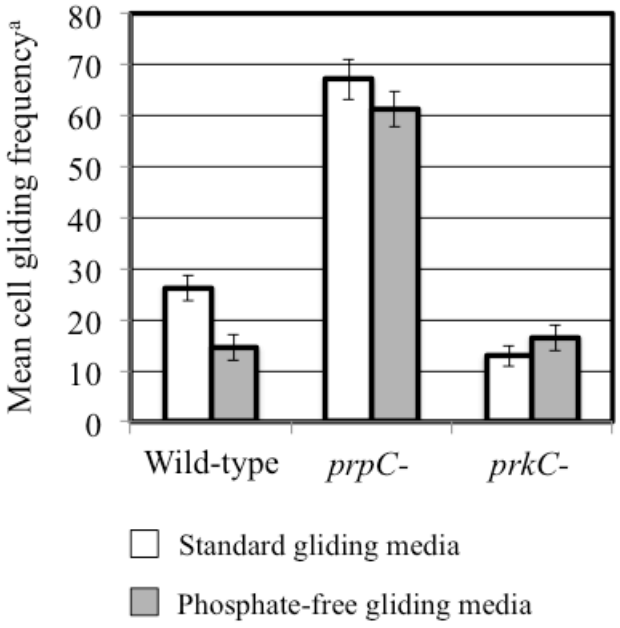

[a] Percentage of cells gliding during observation period ± 95% confidence interval

The identification of PrpC as an important component of the *M. pneumoniae* phosphotransferase system (PTS), specifically involved in the induction of glycerol metabolism (Halbedel *et al.*, 2006) introduced the possibility that the replacement of glucose with glycerol as a carbon source might have detectable effects on gliding in the *prpC* mutant. Both wild-type and the *prpC* mutant exhibited reduced gliding frequencies following replacement of SP-4 growth media with a glycerol gliding media, with wild-type gliding frequency reduced by approximately half that observed in standard gliding media, and 247-100 gliding frequencies reduced by two-thirds. The decrease in *prpC* mutant gliding frequency recovered after 2 hours of incubation, increasing to a level comparable to 247-100 cells in standard gliding media at the same time-point (Fig. 12).

Given the sharp increase in gliding frequency in complemented transformants of 248-377, it seemed likely that increased expression of *prkC* in wild-type might result in a comparable increase in gliding frequency. Transformation of wild-type *M. pneumoniae* with a vector carrying a recombinant copy of MPN248 (the same recombinant transposon was used to complement the *prkC* mutant) resulted in an increase in gliding frequency comparable to the increase detected in the *prpC* mutant (Fig. 13).

Fig. 12. Analysis of wild-type and *prpC* mutant gliding frequencies in glycerol gliding media.

Error bars represent a 95% confidence interval.

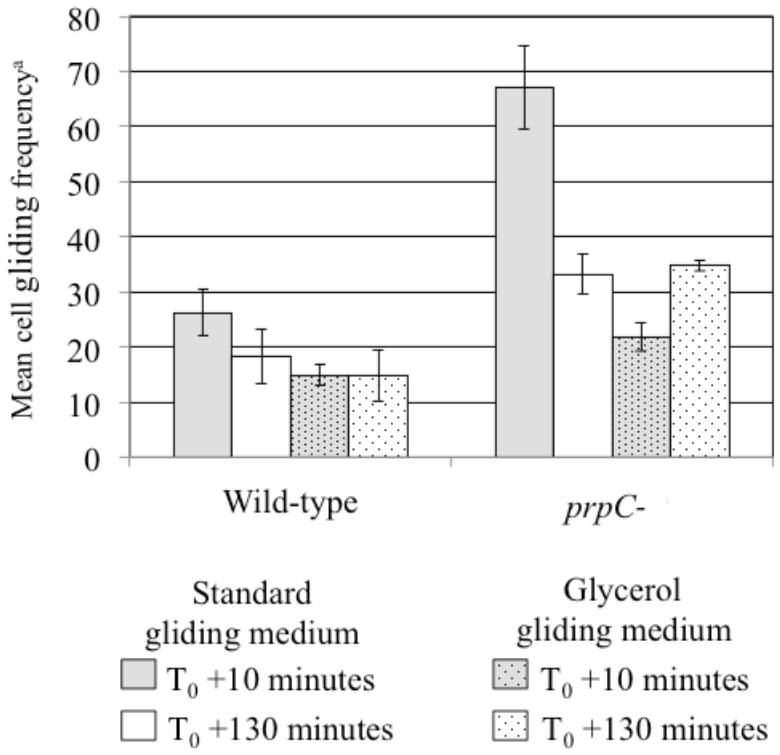

[a] Percentage of cells gliding during observation period ± 95% confidence interval

Fig. 13. Analysis of gliding motility in wild-type with increased expression of *prkC*.

Error bars represent a 95% confidence interval.

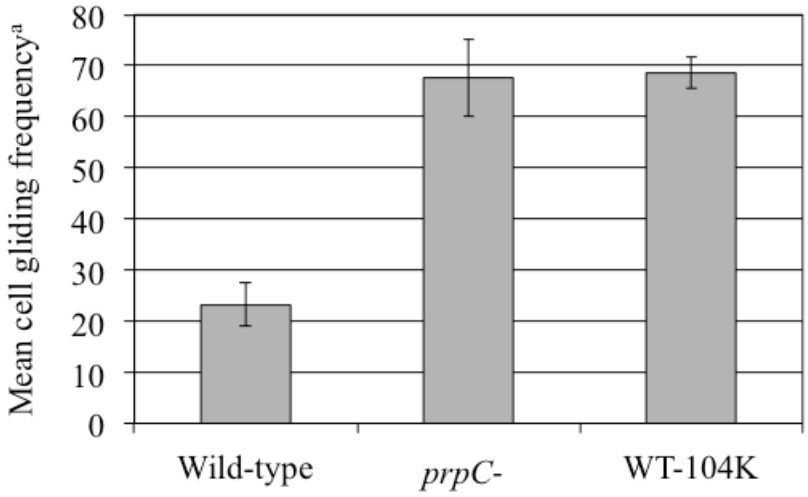

[a]Percentage of cells gliding during observation period ± 95% confidence interval

CHAPTER 5

DISCUSSION

The terminal organelle of *M. pneumoniae* is essential for attachment to the host epithelium (Hu *et al*., 1982), gliding motility (Hasselbring *et al*., 2007a) and cell division (Hasselbring *et al*., 2006a). These factors are themselves dependent on a group of proteins, most significantly the primary and accessory adhesins P1 and P30 (Krause *et al*., 1982 and Baseman *et al*., 1987), the cytoskeletal protein P41, which secures the terminal organelle to the cell body (Hasselbring, 2007a), and along with its accessory protein P24, is required for proper development of new terminal organelles (Hasselbring *et al*., 2007b). The supporting architecture for the localization of these proteins includes the cytoskeletal proteins HMW1, HMW2, HMW3, P200, B, C, and P65, among others, and assembles in a co-dependent process (Krause and Balish, 2004), assisted by the chaperone protein TopJ (Cloward and Krause, 2009). While cytadherence is a constitutive cellular process in *M. pneumoniae* during colonization of host epithelia, and the association between the initiation and cessation of gliding and cell division is well understood, the means by which gliding motility is regulated was not directly studied prior to the isolation of mutants in which the ORFs MPN247, MPN248 and MPN254 were disrupted by transposon insertion.

These mutants were recognized as altered in gliding due to a common aberrant satellite growth phenotype, in which the microcolonies that are commonly observed in

the growth of wild-type *M. pneumoniae* cultures in monolayer developed slowly, never reaching the size of wild-type microcolonies (Fig. 2, Table 3). Additionally, the mutants 247-100 and 254-70 were noted for "constant spreading" of cells away from centers of higher cell density. This satellite growth phenotype, described as "lawn-like", was initially considered to be reflective of reduced gliding frequency and velocity in each mutant (Hasselbring *et al*., 2006b).

The improved gliding assay described in Chapter 3 contradicted this presumption, given that mutant 247-100 actually glides more than twice as frequently as wild-type and at a significantly increased velocity, while 248-377 glides approximately half as frequently as wild-type, and the gliding phenotype of 254-70 is indistinguishable from that of wild-type[1] (Fig. 6). Discrepant gliding phenotypes in mutants with similar colony morphologies are actually not without precedent; Hunnicutt and McBride (2000) found that a majority of transformants with altered satellite growth in *F. johnsoniae* did not exhibit reduced gliding when individual cells were quantitatively evaluated. This suggests that factors leading to altered colony morphology might be only tangentially related to gliding or may result from more subtle phenotypic effects. Additionally, the genomic proximity of MPN247, MPN248 and MPN254 introduces the possibility that all three genes contribute to wild-type microcolony development. This possibility is further suggested by the homology of MPN247 and MPN248 to eSTPs and eSTKs (Dandekar *et al*., 2000, Pereira *et al*., 2011 and Fig. 14) and of MPN254 to a gene implicated in genetic competence induction (CinA) in *S. pneumoniae* (Lee and Morrison, 1999). The potential

[1] Following the finding that *cinA* (MPN254) mutants did not have altered gliding frequencies or velocities, studies were discontinued to focus on the phenotypes of 247-100 and 248-377.

role of each of these gene products in intra- and extracellular signaling outlined a hypothesis worthy of more study.

The contrasting gliding phenotypes of mutants 247-100 and 248-377 strongly suggested a connection between protein phosphorylation and gliding motility in *M. pneumoniae* and furthermore suggested an up- / down-regulation of gliding by PrkC and PrpC, respectively. The effect of phosphorylation on gliding was most clearly seen in the frequency at which cells glide, though an increase in gliding speed was also observed in the PrpC mutant 247-100. This increase in speed was somewhat suspect, given that the PrkC mutant 248-377 was not subject to an attendant decrease in speed along with its decrease in gliding frequency. The possibility exists that the higher proportion of non-motile cells in a wild-type field relative to a field of *prpC* mutant cells created more obstacles for gliding cells, which could result in slower cumulative speeds. Therefore, these data suggest that phosphorylation has a role in the activation of the gliding motor, but not the speed at which the gliding motor propels the cell.

A series of additional experiments that investigated more subtle aspects of gliding motility was attempted following initial characterization of gliding in 247-100 and 248-377. The replacement of standard gliding medium with a phosphate-free gliding medium provided further evidence that PrkC functions in the up-regulation of gliding. In the absence of a phosphate source, wild-type cells glided at a frequency comparable to 248-377. There was no detectable effect on gliding in either mutant, however. This may be due to the inability of 248-377 to deliver phosphates to proteins involved in the

Fig. 14. Clustal alignment of the amino acid sequence of the *M. pneumoniae* PrkC catalytic domain with the catalytic domain of PkA, a homologous kinase from *Mus musculus* (Larkin *et al*, 2007).

Secondary structure notation is based on crystal structure analysis (Zheng *et al*, 1993) in the case of PkA and *in silico* prediction in the case of PrkC (Rost *et al*, 2003).

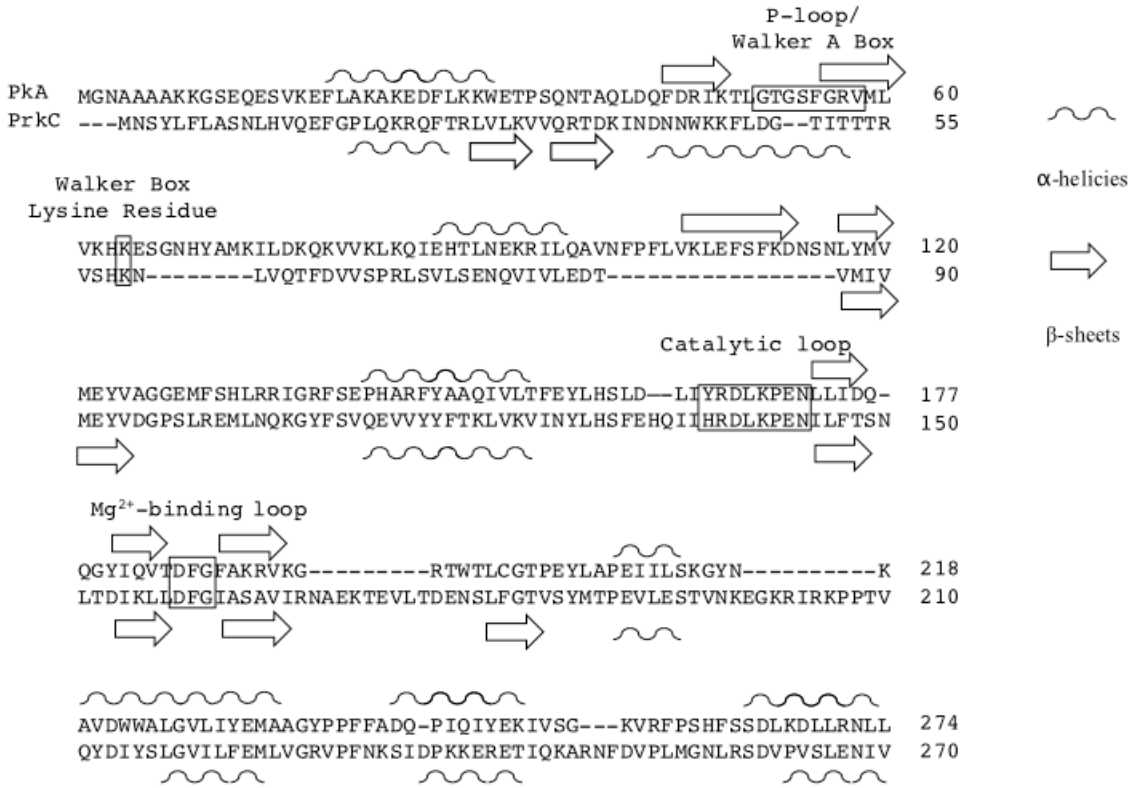
P-loop/
Walker A Box
PkA MGNAAAAKKGSEQESVKEFLAKAKEDFLKKWETPSQNTAQLDQFDRIKTLGTGSFGRVML 60
PrkC ---MNSYLFLASNLHVQEFGPLQKRQFTRLVLKVVQRTDKINDNNWKKFLDG--TITTTR 55
α-helicies
Walker Box
Lysine Residue
VKHKESGNHYAMKILDKQKVVKLKQIEHTLNEKRILQAVNFPFLVKLEFSFKDNSNLYMV 120
VSHKN--------LVQTFDVVSPRLSVLSENQVIVLEDT-----------------VMIV 90
β-sheets
Catalytic loop
MEYVAGGEMFSHLRRIGRFSEPHARFYAAQIVLTFEYLHSLD--LIYRDLKPENLLIDQ- 177
MEYVDGPSLREMLNQKGYFSVQEVVYYFTKLVKVINYLHSFEHQIIHRDLKPENILFTSN 150
Mg2+-binding loop
QGYIQVTDFGFAKRVKG---------RTWTLCGTPEYLAPEIILSKGYN----------K 218
LTDIKLLDFGIASAVIRNAEKTEVLTDENSLFGTVSYMTPEVLESTVNKEGKRIRKPPTV 210
AVDWWALGVLIYEMAAGYPPFFADQ-PIQIYEKIVSG---KVRFPSHFSSDLKDLLRNLL 274
QYDIYSLGVILFEMLVGRVPFNKSIDPKKERETIQKARNFDVPLMGNLRSDVPVSLENIV 270

initiation of gliding and conversely, the inability of 247-100 to dephosphorylate these proteins (Fig. 11).

A similar experiment was suggested by a study identifying PrpC as a component of the PTS of *M. pneumoniae*, functioning in metabolic adjustment to new carbon sources, glycerol in particular (Halbedel *et al.*, 2006). The replacement of glucose with glycerol in gliding media resulted in an immediate decrease in gliding frequency for both wild-type and 247-100, though the mutant strain experienced a sharper decrease proportionally. The gliding frequency of wild-type cells remained constant over a two-hour incubation period, while the gliding frequency of 247-100 increased over the same interval, eventually matching the gliding frequency of 247-100 cells in standard gliding medium (Fig. 12). While these findings are difficult to interpret, it does seem likely that the function of PrpC in the regulation of gliding and in carbon metabolism are integrated.

Finally, the delivery of a second copy of MPN248 via a recombinant transposon designed to complement 248-377 resulted in an increase in gliding frequency comparable to that detected in 247-100. This experiment provided further evidence that phosphorylation by PrkC is an important factor in the initiation and/or the continuation of gliding (Fig. 13).

The reduced attachment detected in quantitative hemadsorption experiments may be attributable to the increased gliding frequency of 247-100 (Fig. 4). In gliding inhibition experiments, the addition of a P1-specific monoclonal antibody to gliding cells resulted in the cessation of gliding, as well as detachment of gliding cells from the chamber slide, while non-motile cells remained attached, suggesting that displacement of P1 was an important factor in gliding (Seto *et al*., 2005a). Similarly, the higher total

number of gliding cells resulting from disruption of MPN247 may have contributed to a lower percent retention.

The finding that 247-100 and 248-377 featured contrasting gliding phenotypes was particularly intriguing in light of the contrasting biochemical functions of the eSTP PrpC and eSTK PrkC in *B. subtilis*, in which these enzymes are known to reversibly phosphorylate elongation factor Tu (EF-Tu) and the ribosome-associated GTPase CpgA. These enzymes and their substrates constitute part of a larger regulatory network that also includes the PrkC-phosphorylated EF-G, and functions in the coordination of cell wall expansion and growth and the germination of *B. subtilis* spores (Absalon *et al*., 2009 and Shah *et al*., 2008). Two methods were used to assess the phosphorylation profiles of 247-100 and 248-377 and thereby identify possible phosphoprotein targets of PrpC and PrkC in *M. pneumoniae*: incorporation of radiolabeled phosphate during growth, followed by electrophoresis, blotting and autoradiography, and Pro Q Diamond staining of protein profiles following electrophoresis.

Pro Q Diamond staining experiments reflected the protein phosphorylation profiles described in *B. subtilis prpC* and *prkC* mutants, in which the phosphorylation profiles of a *prpC* mutant featured evident hyperphosphorylation, while those of a *prkC* mutant showed reduced levels of phosphorylation. The terminal organelle proteins HMW1 and HMW2, previously established as phosphoproteins by $H_3{}^{32}PO_4^-$ incorporation during growth and by cell-free extract experiments (Dirksen *et al*., 1994 and Krebes *et al*., 1995) were among the phosphoproteins that appeared to be subject to phosphorylation and dephosphorylation by PrpC and PrkC in *M. pneumoniae* (Figs. 8B and 9A). The adhesin P1 was also hyperphosphorylated in 247-100, though it was

phosphorylated at wild-type levels in 248-377 (Figs. 8B and 9A). This may be attributable to several factors, such as P1 autophosphorylation or phosphorylation by an unknown protein kinase. Alternatively, PrkC truncation in 248-377 may limit the activity of PrkC or the accessibility of PrkC to HMW1 and HMW2 but not P1. The question of phosphorylation/dephosphorylation of P1 by PrkC and PrpC is further complicated by the fact that the N-terminus and midsection of P1 (the amino acid sequences of which contain the majority of predicted phosphoserine and phosphothreonine resides), are predicted to localize to the cell surface, while PrpC and the catalytic domain of PrkC are predicted to be cytoplasmic (Fig. 15). Collectively, these data suggest a positive correlation between phosphorylation of terminal organelle proteins and gliding frequency in *M. pneumoniae*, albeit by an unknown

While $H_3{}^{32}PO_4^-$ incorporation experiments did not confirm these phenotypes (Fig. 7), we anticipate that radiolabeled phosphoprotein profiles similar to those detected by Pro-Q Diamond staining would be observed by culturing strains with $H_3{}^{32}P0_4^-$ in the initial growth medium, ensuring more time for incorporation, but the necessary phosphate limitation step is problematic with longer incubations (unpublished data).

An especially interesting and unexpected finding here was the detection of hyperphosphorylation of P1 in the HMW1 mutant M6 (Figs. 7 and 8B), which suggests that P1 may be intermediate in the PrkC-dependent phosphorylation of HMW1 and/or HMW2. However, if this were the case P1 might also be expected to be hyperphosphorylated in mutant H9, where HMW2 is absent and HMW1 is present at greatly reduced levels, but this was not the case. Furthermore, the absence of P1 in

Fig. 15. Schematic detailing possible localization of PrkC and adhesin P1.

A. A simplified diagram of the *M. pneumoniae* terminal organelle emphasizing the cell membrane, core and bowl structure and proteins PrkC and P1.

B. Predicted localization of PrkC and P1, based on transmembrane domain prediction (Hofmann and Stoffel, 1993, Czerso *et al*, 1997), sequence alignment (Larkin *et al*, 2007) and phospho-amino acid prediction (Rost *et al*, 2003).

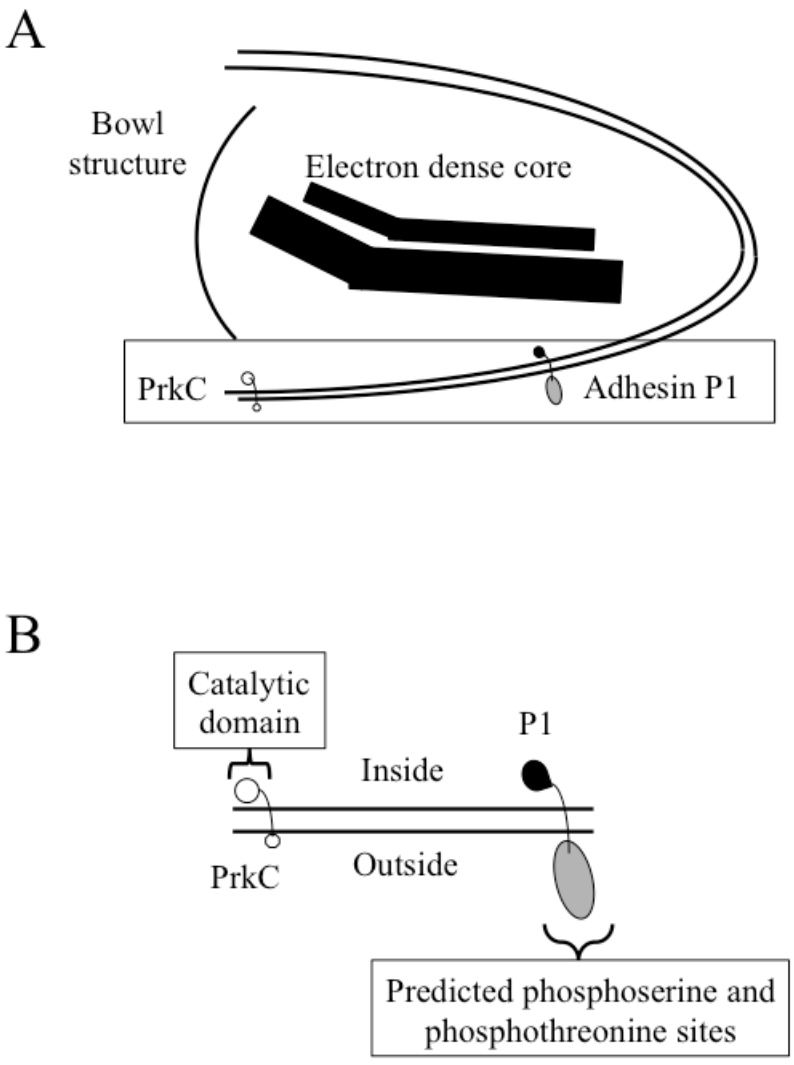
A
Bowl
structure
Electron dense core
PrkC
Adhesin P1
B
Catalytic
domain
P1
Inside
PrkC
Outside
Predicted phosphoserine and
phosphothreonine sites

mutant IV-22 (Fig. 8B) did not affect HMW1 or HMW2 phosphorylation levels. An alternate explanation for P1 hyperphosphorylation is suggested by the improper cellular localization of P1 in M6 mutant cells (Hahn *et al*., 1998); where PrkC may simply have more access to P1 when it is not localized to the terminal organelle, but again if this were the case then P1 should also be hyperphosphorylated in mutant H9. The M6 mutant also has a truncated terminal organelle protein P30 (Layh-Schmitt *et al*., 1995), which might also account for P1 hyperphosphorylation in this mutant. This possibility is testable by examining P1 phosphorylation in mutant II-7, which has a similarly truncated P30 protein, as well as in mutant M6 complemented with recombinant wild-type alleles for P30 and HMW1.

Complementation of 247-100 and 248-377 confirmed that the mutant gliding phenotypes and phosphorylation profiles observed in these mutants were indeed the result of transposon insertions in MPN247 and MPN248. The increased gliding frequency and velocity of 247-100 was restored to the wild-type standard in complemented transformants, while phosphoprotein bands hyperphosphorylated in the mutant strain (HMW1, HMW2 and P1) were reduced in intensity relative to wild-type (Fig. 6, 8B and 9A). Wild-type satellite growth also returned in complemented transformants of 247-100 (Fig. 2, Table 3). Gliding frequency was increased well above the wild-type standard in complemented transformants of 248-377, while phosphoprotein bands of reduced intensity in the mutant strain were hyperphosphorylated following complementation (Fig. 6, 8B and 9A). Wild-type satellite growth was not detected in complemented transformants of 248-377.

The hyperphosphorylation and increased gliding frequency detected in 248-377 CT1 and 248-377 CT2 may be attributable to the phosphorylation by truncated PrkC in these strains, combined with the catalytic activity of transposon-delivered, recombinant wild-type *prkC*. The entire predicted catalytic domain of PrkC is present in the mutant 248-377 (Fig.1, Fig. 14), along with all but 12 amino acids of the C-terminus of the enzyme, which are predicted to localize extracelluarly (Fig. 15). In other eSTKs, extracellular domains are required for the activation of the catalytic domain, in which ligand binding by these domains is followed by homodimerization of kinase molecules and autophosphorylation (Ortiz-Lombardia *et al*., 2003 and Young *et al*., 2003). If this is also the case in *M. pneumoniae*, the addition of wild-type PrkC may result in some recovery of function for truncated PrkC molecules, leading to hyperphosphorylation of terminal organelle proteins and an increase in gliding frequency.

In their analysis of similar mutants, Schmidl and colleagues (2009) described some variances in mutant phenotypes. Most significantly, the *prkC* mutant *prkC:Tn* exhibits reduced steady state levels of several proteins involved in attachment and cytadherence, including HMW1 and HMW2, the latter of which was completely absent when assessed by Western immunoblotting. The authors attribute this to a role for PrkC phosphorylation in the stability of these proteins. The wild-type levels of the same proteins in mutant 248-377 would seem to contradict this result, though the copy of PrkC in mutant 248-377 does not lack the predicted catalytic domain as does *prkC:Tn*. Mutant 248-377 may be capable of phosphorylating HMW2 and other target phosphoproteins to a degree sufficient to maintain their stability at wild-type levels. It is also possible that the "haystack mutagenesis" method of Schmidl and colleagues is more likely than simple

transposon mutagenesis to yield spontaneous secondary mutations given its reliance on multiple passages to select for particular mutants. The reduced steady state levels of HMW1, HMW3, P65, P41 and P28 seen in the *prkC:Tn* mutant are consistent with the protein profiles of the HMW2 mutants I-2 and H9 (Fisseha *et al*., 1999, Hedreyda and Krause, 1995). Finally, the hyperphosphorylation of HMW2 detected in the *prpC* mutant 247-100 is not seen in mutant *prpC:Tn*. This may simply be attributable to differences in biologically available phosphate in the SP-4 medium used here as compared to the Hayflick's broth used by Schmidl and colleagues.

While reversible protein phosphorylation of terminal organelle proteins by the kinase/phosphatase pair of PrkC and PrpC is clearly associated with gliding motility in *M. pneumoniae*, this dissertation does not identify specific phosphoproteins as components of the gliding motor or assert that protein phosphorylation by PrkC drives the gliding motor. Rather, we suggest that PrpC and PrkC constitute part of a regulatory circuit comparable to the system in *B. subtilis* described by Absalon and colleagues, wherein phosphorylation of elongation factor Tu and other phosphoproteins influences aspects of sporulation and cell wall biosynthesis. Regulation of swarming in *Myxococcus xanthus*, cell division in *Mycobacterium tuberculosis* and virulence factor expression in *Yersinia pseudotuberculosis* by homologous eSTKs and eSTPs have been previously reported (Pereira *et al*., 2011), indicating that reversible phosphorylation is coupled to a multiple functions in bacteria. Gliding motility in *M. pneumoniae* is a strong candidate for inclusion in the growing category of cellular processes controlled in part by reversible serine / threonine phosphorylation.

REFERENCES

Absalon, C., M. Obuchowski, E. Madec, D. Delattre, I. B. Holland and S. J. Seror. 2009. CpgA, EF-Tu and the stressosome protein YezB are substrates of the Ser/Thr kinase/phosphatase couple, PrkC/PrpC, in *Bacillus subtilis*. Microbiology. **155:** 932-943.

Bakal, C. J., and J. E. Davies. 2000. No longer an exclusive club: eukaryotic signalling domains in bacteria. Trends Cell Biol. **10:** 32–38.

Balish, M.F., R. T. Santurri, A.M. Ricci, K.K. Lee, and D. C. Krause. 2003. Localization of *Mycoplasma pneumoniae* cytadherence-associated protein HMW2 by fusion with green fluorescent protein: implications for attachment organelle structure. *Mol Microbiol* **47**: 49-60.

Barthe, P., G. V. Mukamolova, C. Roumestand, and M. Cohen-Gonsaud. 2010. The structure of PknB extracellular PASTA domain from *Mycobac- terium tuberculosis* suggests a ligand-dependent kinase activation. Structure **18:** 606–615.

Baseman, J.B., R. M. Cole., D. C. Krause, and D. K. Leith. 1982. Molecular basis for cytadsorption of *Mycoplasma pneumoniae*. J Bacteriol **151**: 1514-1522.

Baseman, J.B., J. Morrison-Plummer., D. Drouillard, B. Puleo-Scheppke, V. V. Tryon, and S. C. Holt. 1987. Identification of a 32-kilodalton protein of *Mycoplasma pneumoniae* associated with hemadsorption. Isr J Med Sci **23**: 474-479.

Biberfield, G., and P. Biberfield. 1970. Ultrastructural Features of *Mycoplasma pneumoniae*. J Bacteriol **102**: 855-861.

Bordet, J. 1910. La morphologie du microbe de la peripneumonie des bovides. Ann. Inst. Pasteur. **24:** 168-179.

Bose S. R., M. F. Balish and D. C. Krause. 2009. *Mycoplasma pneumoniae* cytoskeletal protein HMW2 and the architecture of the terminal organelle. J. Bacteriol. **191:** 6741-6748.

Bredt, W. 1968. Motility and multiplication of *Mycoplasma pneumoniae*. A phase contrast study. Pathol Microbiol **32**: 321-326.

Bredt, W. 1973. Motility of Mycoplasmas. *Annals of the New York Academy of Sciences*. **225:** 246–250.

Brown, D. R. 2002. Mycoplasmosis and immunity of fish and reptiles. Front Biosci. **7**: 1338-1346.

Brown, D. R., R. F. Whitcomb, and J. M. Bradbury. 2007. Revised minimal standards for description of new species of the class *Mollicutes* (division *Tenericutes*). IJSEM. **57:** 2703-2719.

Chanock, R.M., L. Hayflick, L., and M.F. Barile. 1962. Growth on artificial medium of an agent associated with atypical pneumonia and its identification as a PPLO. Proc Natl Acad Sci U S A. **48**: 41-49.

Cloward, J. M. and D. C. Krause. 2009. *Mycoplasma pneumoniae* J-domain protein required for terminal organelle function. Mol. Microbiol. **71:** 1296-1307.

Clyde, W. V. A. 1979. *Mycoplasma pneumoniae* infections of man. In *The Mycoplasmas*, I. (ed .J.G. Tully and R. F. Whitcomb), pp. 275-303. New York: Academic Press.

Clyde, W. V. A. 1993. Clinical overview of typical *Mycoplasma pneumoniae* infections.

Clin Infect Dis. **17:** S32-36.

Cohen, G. and N. L. Somerson. 1967. *Mycoplasma pneumoniae*: hydrogen peroxide secretion and its possible role in virulence. Ann. NY Acad. Sci. **143:** 85-87.

Collier, A.M., and Clyde, W.A. (1974) Appearance of *Mycoplasma pneumoniae* in lungs of experimentally infected hamsters and sputum from patients with natural disease. Am Rev Respir Dis. **110**: 765-773.

Cserzo M., E. Wallin, I. Simon, G. von Heijne and A. Elofsson. 1997. Prediction of transmembrane alpha-helices in procariotic membrane proteins: the Dense Alignment Surface method. Prot. Eng. **10:** 673-676.

Dandekar, T., M. Huynen, J. T. Regula, B. Ueberle, C. U. Zimmermann, M. A. Andrade, T. Doerks, L. Sanchez-Pulido, B. Snel, M. Suyama, Y. P. Yuan, R. Herrmann, and P. Bork. 2000. Re-annotating the *Mycoplasma pneumoniae* genome sequence: adding value, function and reading frames. Nucleic Acids Res. **28:**3278-3288.

De Verdier, C. H. 1952. Isolation of phosphothreonine from bovine casein. Nature **170:** 804–805.

Dirksen, L. B., K. A., and D. C. Krause. 1994. Phosphorylation of cytadherence-accessory proteins in *Mycoplasma pneumoniae*. J. Bacteriol. **176:**7499-7505.

Eaton, M. D., G. Meiklejohn, W. van Herick, and M. Corey. 1945. Studies on the etiology of primary atypical pneumonia. II. Properties of the virus isolated and propagated in chick embryos. J. Exp. Med. **82:** 329-342.

Edward, D. G. and E. A. Freundt. 1956. The classification and nomenclature of organisms of the pleuropneumonia group. J. Gen. Microbiol. **14:** 197-207.

Elford, W. J. 1929. Ultra-filtration methods and their application in bacteriological and pathological studies. Brit. J. Exptl. Path. **10**: 126-144.

Feldner, J., U. Gobel, and W. Bredt. 1982. *Mycoplasma pneumoniae* adhesin localized to tip structure by monoclonal antibody. Nature **298**: 765-767.

Ferwerda, A., H. A. Moll, and R. de Groot. 2001. Respiratory tract infections by *Mycoplasma pneumoniae* in children: a review of diagnostic and therapeutic measures. Eur. J. Pediatr. **160:** 483-491.

Fisseha, M., H. W. Gohlmann, R. Herrmann, and D. C. Krause. 1999. Identification and complementation of frameshift mutations associated with loss of cytadherence in *Mycoplasma pneumoniae*. J. Bacteriol. **181:** 4404-4410.

Fraser, C.M., Gocayne, J.D., White, O., Adams, M.D., Clayton, R.A., Fleischmann, R.D., Bult, C.J., Kerlavage, A.R., Sutton, G., Kelley, J.M., et al. 1995. The minimal gene complement of *Mycoplasma genitalium*. Science. **270**: 397-403.

Galperin, M. Y., R. Higdon, and E. Kolker. 2010. Interplay of heritage and habitat in the distribution of bacterial signal transduction systems. Mol. Biosyst. **6:**721–728.

Garnak, M., and H. C. Reeves. 1979. Phosphorylation of isocitrate dehy- drogenase of *Escherichia coli*. Science **203:** 1111–1112.

Glass, J. I., N. Assad-Garcia, N. Alperovich, M. Yooseph, M. R. Lewis, M. Maruf, C. A. Hutchison III, H. O. Smith, and J. C. Venter. 2006. Essential genes of a minimal bacterium. Proc. Natl. Acad. Sci. U.S.A. **103:** 425-430.

Gobel, U., V. Speth, and W. Bredt. 1981. Filamentous structures in adherent *Mycoplasma pneumoniae* cells treated with nonionic detergents. J. Cell Biol. **91:**537-543.

Goldman, *et al.* 2006. Evolution of sensory complexity recorded in a myxobacterial genome. Proc Natl Acad Sci U S A. **103:** 15200-15205.

Glass, J. I., N. Assad-Garcia, N. Alperovich,S. Yooseph, M. R. Lewis, M. Maruf, C. A. Hutchison III, H. O. Smith, and J. C. Venter. 2006. Essential genes of a minimal bacterium. Proc. Natl. Acad. Sci. U.S.A. **103:** 425-430.

Hahn, T. W., K. A. Krebes, and D. C. Krause. 1996. Expression in *Mycoplasma pneumoniae* of the recombinant gene encoding the cytadherence-associated protein HMW1 and identification of HMW4 as a product. Mol. Microbiol. **19:**1085-1093.

Hahn, T. W., M. J. Willby, and D. C. Krause. 1998. HMW1 is required for cytadhesin P1 trafficking to the attachment organelle in *Mycoplasma pneumoniae*. J. Bacteriol. **180:** 1270-1276.

Hahn, T.W., E. A. Mothershed, R. H. Waldo, and D. C Krause. 1999. Construction and analysis of a modified Tn*4001* conferring chloramphenicol resistance in *Mycoplasma pneumoniae*. Plasmid **41**: 120-124.

Halbedel, S., J. Busse, S. R. Schmidl, and J. Stülke. Regulatory protein phosphorylation in *M. pneumoniae*. A PP2C-type phosphatase serves to dephosphorylate HPr (Ser~P). J Biol Chem. **281:** 26253-26259.

Hardy R.D., J. J. Coalson, J. Peters, A. Chaparro, C. Techasaensiri, A. M. Cantwell, T. R. Kannan, J. B. Baseman, and P. H. Dube. 2009. Analysis of Pulmonary Inflammation and Function in the Mouse and Baboon after Exposure to *M. pneumoniae* CARDS Toxin. PLoS One. **4.**

Hasselbring, B. M., J. L. Jordan, and D. C. Krause. 2005. Mutant analysis reveals a specific requirement for protein P30 in *Mycoplasma pneumoniae* gliding motility. J. Bacteriol. **187:** 6281-6289.

Hasselbring B. M., J. L. Jordan, R. W. Krause, D. C. Krause. 2006a. Terminal organelle development in the cell wall-less bacterium *Mycoplasma pneumoniae*. Proc. Natl. Acad. Sci. USA. **103**: 16478-16483.

Hasselbring B. M., C. A. Page, E. S. Sheppard, and D. C. Krause. 2006b. Transposon mutagenesis identifies genes associated with *Mycoplasma pneumoniae* gliding motility. J. Bacteriol. **188:** 6335-6345.

Hasselbring B. M. and D. C. Krause. 2007. Cytoskeletal protein P41 is required to anchor the terminal organelle of the wall-less prokaryote *Mycoplasma pneumoniae*. Mol Microbiol. **63:** 44-53.

Hayflick, L. 1965. Tissue cultures and mycoplasmas. Tex. Rep. Biol. Med. **23:**Suppl 1:285+.

Hedreyda, C. T., K. K. Lee, and D. C. Krause. 1993. Transformation of *Mycoplasma pneumoniae* with Tn*4001* by electroporation. Plasmid **30:**170-175.

Hedreyda C. T., and D. C. Krause. 1995. Identification of a possible cytadherence regulatory locus in *Mycoplasma pneumoniae*. Infect Immun. **63:** 3479-3483.

Henderson, G. P., and G. J. Jensen. 2006. Three-dimensional structure of *Mycoplasma pneumoniae*'s attachment organelle and a model for its role in gliding motility. Mol. Microbiol. **60:**376-385.

Henz S. R., D. H. Huson, A. F. Auch, K. Nieselt-Struwe and S. C. Schuster. 2003 Whole-genome prokaryotic phylogeny. Bioinformatics **21:** *2329–2335*

Himmelreich, R., H. Hilbert, H. Plagens, E. Pirkl, B. C. Li, and R. Herrmann. 1996. Complete sequence analysis of the genome of the bacterium *Mycoplasma pneumoniae*. Nucleic Acids Res. **24:**4420-4449.

Hodges, G. R., and R. L. Perkins. 1969. Landry-Guillain-Barré Syndrome Associated With Mycoplasma pneumoniae Infection. JAMA. **210:** 2088-2090.

Hofmann, K. and W. Stoffel. 1993. TMbase - A database of membrane spanning proteins segments.Biol. Chem. **374:** 166

Hu, P.C., Collier, A.M., and Baseman, J.B. 1977. Surface parasitism by *Mycoplasma pneumoniae* of respiratory epithelium. J Exp Med **145:** 1328-1343.

Inamine, J. M., S. Loechel, and P. C. Hu. 1988. Analysis of the nucleotide sequence of the P1 operon of *Mycoplasma pneumoniae*. Gene. **73:** 175-183.

Inamine, J. M., T. P. Denny, S. Loechel, and P. C. Hu. 1990. Evidence that UGA is read as a tryptophan codon rather than as a stop codon by *Mycoplasma pneumoniae*, *Mycoplasma genitalium*, and *Mycoplasma gallisepticum*. J. Bacteriol. **172:** 504-506.

Iwanicki, A., A. Herman-Antosiewicz, M. Pierechod, S. J. Seror, and M. Jacobs, E. 2002. *Mycoplasma pneumoniae* disease manifestations and epidemiology, p. 519-530. *In* Razin, S. and R. Herrmann (eds.). *Molecular Biology and Pathogenicity of Mycoplasmas*, Kluwer Academic/Plenum, NY.

Jordan J. L., H. Y. Chang, M. F. Balish, L. S. Holt, S. R. Bose, B. M. Hasselbring, R. H. Waldo 3rd, T. M. Krunkosky, D. C. Krause. 2007. Protein P200 is dispensable for

Mycoplasma pneumoniae hemadsorption but not gliding motility or colonization of differentiated bronchial epithelium. Infect Immun. **1**: 518-22.

Kannan, T.R. and J. B. Baseman. 2006. ADP-ribosylating toxin and vacuolating cytotoxin of *Mycoplasma pneumoniae* represents unique virulence determinant. Proc Natl Acad Sci USA. **17:** 6724-6729.

Kannan T.R., J. J. Coalson, M. Cagle, O. Musatovova, R. D. Hardy RD, and J. B. Baseman. Synthesis and Distribution of CARDS Toxin During *Mycoplasma pneumoniae* infection in a murine model. J. Infect. Dis. **10:** 1596-1604.

Kennelly, P. J. 2002. Protein kinases and protein phosphatases in prokaryotes: a genomic perspective. FEMS Microbiol. Lett. **206:**1–8**.**

Knudtson, K. L., and F. C. Minion. 1993. Construction of Tn4001lac derivatives to be used as promoter probe vectors in mycoplasmas. Gene **137:**217-222.

Krause, D.C., Leith, D.K., Wilson, R.M., and Baseman, J.B. 1982. Identification of *Mycoplasma pneumoniae* proteins associated with hemadsorption and virulence. Infect Immun. **35**: 809-817.

Krause, D.C., and J.B. Baseman. 1983. Inhibition of *Mycoplasma pneumoniae* hemadsorption and adherence to respiratory epithelium by antibodies to a membrane protein. Infect Immun **39**: 1180-1186.

Krause, D. C., T. Proft, C. T. Hedreyda, H. Hilbert, H. Plagens, and R. Herrmann. 1997. Transposon mutagenesis reinforces the correlation between *Mycoplasma pneumoniae* cytoskeletal protein HMW2 and cytadherence. J. Bacteriol. **179:** 2668-2677

Krause, D. C., and M. F. Balish. 2004. Cellular engineering in a minimal microbe: structure and assembly of the terminal organelle of *Mycoplasma pneumoniae*. Mol. Microbiol. **51:** 917-924.

Krebes K. A., L. B. Dirksen and D. C. Krause. 1995. Phosphorylation of *Mycoplasma pneumoniae* cytadherence-accessory proteins in cell extracts. J. Bacteriol. **177:** 4571-4574.

Krishnakumar, R., N. Assad-Garcia, G. A. Sanders, Q. Phan, M. G. Montague and J. I. Glass. 2010. Targeted chromosomal knockouts in *Mycoplasma pneumoniae*. Appl. and Env. Microbiol. **76:** 5297-5299.

Laemmli, U. K. 1970. Cleavage of structural proteins during the assembly of the head of bacteriophage T4. Nature **227:** 680-685.

Larkin M.A., G. Blackshields, N. P. Brown, R. Chenna, P. A. McGettigan, H. McWilliam, F. Valentin, I. M. Wallace, A. Wilm, R. Lopez, J. D. Thompson, T.J. Gibson, D. G. Higgins. 2007. ClustalW and ClustalX version 2. Bioinformatics **23:** 2947–2948.

Layh-Schmitt, G., and R. Herrmann. 1992. Localization and biochemical characterization of the ORF6 gene product of the *Mycoplasma pneumoniae* P1 operon. Infect Immun **60**: 2906-2913.

Layh-Schmitt, G., and R. Herrmann. 1994. Spatial arrangement of gene products of the P1 operon in the membrane of *Mycoplasma pneumoniae*. Infect Immun **62**: 974-979.

Layh-Schmitt, G., H. Hilbert, and E. Pirk. 1995. A spontaneous hemadsorption-negative mutant of *Mycoplasma pneumoniae* exhibits a truncated adhesin-related 30-

kilodalton protein and lacks the cytadherence-accessory protein HMW1. J Bacteriol **177**: 843-846.

Lee, M.S. and D.A. Morrison. 1999. Identification of a new regulator in *Streptococcus pneumoniae* linking quorum sensing to competence for genetic transformation. . J. Bacteriol. **181:** 5004-5016.

Lipman R. B., W. A. Clyde, Jr, and F. W. Denny. 1969. Characteristics of virulent, attenuated, and a virulent *Mycoplasma pneumoniae* strains. J. Bacteriol. **100:** 1037-1043.

Luby, J.P. 1991. Pneumonia Caused by *Mycoplasma pneumoniae* Infection. In *Clinics in Chest Medicine: Atypical Pneumonia Syndromes*. **12**. Winterbauer, R.H. (ed). Philadelphia: W.B. Saunders Company, pp. 237-244.

Maniloff, J. 2002. Phylogeny and Evolution. In *Molecular Biology and Pathogenicity of Mycoplasmas*. Razin, S. and Herrmann, R. (eds). New York: Kluwer Academic/Plenum, pp. 31-43.

Marmion, B. P. and G. M. Goodburn. 1961. Effect of an organic gold salt on Eaton's primary atypical pneumonia agent and other observations. Nature. **189:** 247-248.

McBride *et al.* 2009. Novel Features of the Polysaccharide-Digesting Gliding Bacterium *Flavobacterium johnsoniae* as Revealed by Genome Sequence Analysis. Appl. Environ. Microbiol. **75:** 6864–6875.

Meng, K.E., and R.M. Pfister. 1980. Intracellular structures of *Mycoplasma pneumoniae* revealed after membrane removal. J. Bacteriol. **144**: 390-399.

Munoz-Dorado, J., S. Inouye, and M. Inouye. 1991. A gene encoding a protein serine/threonine kinase is required for normal development of *M. xanthus,* a gram-

negative bacterium. Cell **67:** 995–1006.

Obuchowski, M., E. Madec, D. Delattre, I. Boe, A. Iwanicki, D. Foulger and S. Seror. 2000. Characterization of PrpC from *Bacillus subtilis*, a member of the PPM phosphatase family. J. Bacteriol. **182:** 5634–5638.

Obuchowski. 2002. PrpE, a PPP protein phosphatase from *Bacillus subtilis* with unusual substrate specificity. Biochem. J. **366:** 929–936.

Ortiz-Lombardia, M., F. Pompeo, B. Boitel, and P. M. Alzari. 2003. Crystal structure of the catalytic domain of the PknB serine/threonine kinase from *Mycobacterium tuberculosis*. J. Biol. Chem. **278:** 13094–13100.

Osaki, M., et al. 2009. The StkP/PhpP signaling couple in *Streptococcus pneumoniae:* cellular organization and physiological characterization. J. Bacteriol. **191:** 4943–4950.

Proft, T., and R. Herrmann. 1994. Identification and characterization of hitherto unknown *Mycoplasma pneumoniae* proteins. Mol. Microbiol. **13:**337-348

Proft, T., H. Hilbert, G. Layh-Schmitt, and R. Herrmann. 1995. The proline-rich P65 protein of *Mycoplasma pneumoniae* is a component of the Triton X-100-insoluble fraction and exhibits size polymorphism in the strains M129 and FH. J Bacteriol **177**: 3370-3378.

Proft, T., H. Hilbert, H. Plagens, and R. Herrmann. 1996. The P200 protein of *Mycoplasma pneumoniae* shows common features with the cytadherence-associated proteins HMW1 and HMW3. Gene **171:**79-82

Nakane D., J. Adan-Kubo, T. Kenri, and M. Miyata. 2011. Isolation and characterization of P1 adhesin, a leg protein of the gliding bacterium *Mycoplasma pneumoniae*. J. Bacteriol. **193:** 715-722.

Nocard E., and P. Roux. 1898. Le microbe de la peripneumonie. Ann. Inst. Pasteur. **12:** 240-262.

Pereira S. F. F., L. Goss, and J. Dworkin. 2011. Eukaryote-Like Serine/Threonine Kinases and Phosphatases in Bacteria. Microbiol. and Mol. Biol. Reviews. **75:** 195-212.

Powell, D A.. P.C. Hu, M. Wilson, A. M. Collier, and J. B. Baseman. 1976. Attachment of *Mycoplasma pneumoniae* to respiratory epithelium. Infect Immun **13**: 959-966.

Regula, J.T., G. Boguth., A. Gorg, J. Hegermann, F. Mayer, R. Frank, and R. Herrmann. 2001. Defining the mycoplasma 'cytoskeleton': the protein composition of the Triton X-100 insoluble fraction of the bacterium *Mycoplasma pneumoniae* determined by 2-D gel electrophoresis and mass spectrometry. Microbiology **147**: 1045-1057.

Romero-Arroyo, C. E., J. Jordan, S. J. Peacock, M. J. Willby, M. A. Farmer, and D. C. Krause. 1999. *Mycoplasma pneumoniae* protein P30 is required for cytadherence and associated with proper cell development. J. Bacteriol. **181:**1079-1087.

Rost, B., G. Yachdav and J. Liu. 2004. The PredictProtein server. Nucl. Acids Res. **32:** 321-326.

Sabin, A.B. 1938. Identification of the filterable, transmissible neurolytic agent isolated from *Toxoplasma*-infected tissue as a new pleuropneumonia-like microbe. Science. **88:** 55-56.

Schmidl S. R., K. Gronau, C. Hames, J. Busse , D. Becher, M. Hecker, J. Stülke. 2009. The stability of cytadherence proteins in *Mycoplasma pneumoniae* requires activity of the protein kinase PrkC. Infect Immun. **78:** 184-192.

Schmidl S. R., K. Gronau, N. Pietack, M. Hecker, D. Becher, and J. Stulke. 2010. The Phosphoproteome of the Minimal Bacterium *Mycoplasma pneumoniae*. Mol. Cell. Proteomics. **9:** 1228-1242.

Schmidl S. R., A. Otto, M. Lluch-Senar, J. Pinol, J. Busse, D Becher and J. Stulke. 2011. A trigger enzyme in *Mycoplasma pneumoniae*: impact of the glycerophosphodiesterase GlpQ on virulence and gene expression. PLoS Pathog. **9**.

Seto, S., T. Kenri, T. Tomiyama, and M. Miyata. 2005a. Involvement of P1 adhesin in gliding motility of *Mycoplasma pneumoniae* as revealed by the inhibitory effects of antibody under optimized gliding conditions. *J. Bacteriol*. **187:** 1875-1877.

Seto, S., A. Uenoyama, and M. Miyata. 2005b. Identification of a 521-kilodalton protein (Gli521) involved in force generation or force transmission for *Mycoplasma mobile* gliding. J. Bacteriol. **187:** 3502-3510.

Seybert, A., R. Herrmann and A. S. Frangakis. 2006. Structural analysis of *Mycoplasma pneumoniae* by cryo-electron tomography. J. Structural Biology. **156:** 342-354.

Shah, I.M., M. H. Laaberki, D. L. Popham, and J. Dworkin. 2008. A eukaryotic-like Ser/Thr kinase signals bacteria to exit dormancy in response to peptidoglycan fragments. Cell. **135**: 486-96.

Shapiro, L. and R. Losick. 2000. Dynamic spatial regulation in the bacterial cell. Cell **100**, 89-98.

Shen, B., L. Dong, S. Xiao, and M. Kowalewski. 2008. The Avalon Explosion: Evolution of Ediacara Morphospace. Science. **319:** 81-84.

Sobeslavsky, O., Prescott, B., and Chanock, R. 1968. Adsorption of *Mycoplasma pneumoniae* to neuraminic acid receptors of various cells and possible role in virulence. J Bacteriol **96**: 695-705.

S**perker, B., P. C. Hu, and R. Herrmann.** 1991. Identification of gene products of the P1 operon of *Mycoplasma pneumoniae*. Mol. Microbiol. **5:**299-306

Stevens, M. K., and D. C. Krause. 1991. Localization of the *Mycoplasma pneumoniae* cytadherence-accessory proteins HMW1 and HMW4 in the cytoskeletonlike Triton shell. J. Bacteriol. **173:** 1041-1050.

Stevens, M. K., and D. C. Krause. 1992. *Mycoplasma pneumoniae* cytadherence phase-variable protein HMW3 is a component of the attachment organelle. J. Bacteriol. **174:** 4265-4274.

Su, H., C. A Hutchison III, and M. C. Giddings. 2007. Mapping phosphoproteins in *Mycoplasma genitalium* and *Mycoplasma pneumoniae*. BMC Microbiology. **7.**

Sutherland E. R., and R. J. Martin. 2007. Asthma and Atypical Bacterial Infection. *Chest*. **6:** 62-66.

Talkington, D. F., K. B. Waites, S. B. Schwartz, and R. E. Besser. 2001. Emerging from Obscurity: Understanding Pulmonary and Extrapulmonary Syndromes, Pathogenesis, and Epidemiology of Human *Mycoplasma pneumoniae* Infections, p. 57-82. *In* Scheld, W. M., W. A. Craig, and J. M. Hughes (eds).

Taylor-Robinson, D. 1996. Infections due to species of *Mycoplasma* and *Ureaplasma*: an update. Clin Infect Dis. **23:** 671-682.

Towbin, H., T. Staehelin, and J. Gordon. 1979. Electrophoretic transfer of proteins from polyacrylamide gels to nitrocellulose sheets: procedure and some applications. Proc. Natl. Acad. Sci. USA **76:** 4350-4354

Tully, J. G., R. F. Whitcomb, H. F. Clark, and D. L. Williamson. 1977. Pathogenic mycoplasmas: cultivation and vertebrate pathogenicity of a new spiroplasma. Science **195:** 892-894.

Van Noort, V. ***et al.*** 2012. Cross-talk between phosphorylation and lysine acetylation in a genome-reduced bacterium. Mol. Syst. Biol. **8.**

Waites, K. B., and D. F. Talkington. 2004. *Mycoplasma pneumoniae* and its role as a human pathogen. Clin. Microbiol. Rev. **17:**697-728.

Willby, M.J., and D. C. Krause, 2002. Characterization of a *Mycoplasma pneumoniae hmw3* mutant: implications for attachment organelle assembly. J Bacteriol **184**: 3061-3068.

Wilson, M. H. and A. M. Collier. 1976. Ultrastructural study of *Mycoplasma pneumoniae* in organ culture. *J. Bacteriol*. **125:** 332-339.

Yeats, C., R. D. Finn, and A. Bateman. 2002. The PASTA domain: a beta-lactam-binding domain. Trends Biochem. Sci. **27:** 438.

Young, T. A., B. Delagoutte, J. A. Endrizzi, A. M. Falick, and T. Alber. 2003. Structure of *Mycobacterium tuberculosis* PknB supports a universal activa- tion mechanism for Ser/Thr protein kinases. Nat. Struct. Biol. **10:** 168–174.

Yus *et al.* 2009. Impact of Genome Reduction on Bacterial Metabolism and Its Regulation. Science. **326:** 1263-1268.

Zimmerman, C. U. and R. Herrmann. 2005. Synthesis of a small, cysteine-rich, 29 amino acids long peptide in *Mycoplasma pneumoniae*. FEMS Micro. Letters. **253:** 315-321.

Zheng, J., E. A. Trafny, D. R. Knighton, N. H. Xuong, S. S. Taylor, L. F. Ten Eyck, and J.M. Sowadski. 1993. A refined crystal structure of the catalytic subunit of cAMP-dependent protein kinase complexed with MnATP and a peptide inhibitor. Acta Crystallogr.,Sect.D **49:** 362-365.